Chapter 1

Introduction

Humans use vision as their primary means for gathering information about, and navigating through, their surroundings. Providing this ability to automated systems would be a large step toward having them operate effectively in our world. There are, however, two major obstacles to automated vision: incomplete human knowledge of how to reliably derive high-level information from a 2-D image; and the computational complexity of image processing and analysis methods. The latter is of primary concern in the research and development of real-time systems.

Only recently has the growth in affordable computing power and research into faster techniques allowed some complex vision tasks to move into industrial and consumer applications. Since many of the most compute-intensive image processing operations are also highly parallel they could be accelerated by orders of magnitude using a customized hardware implementation. This is widely recognized in real-time vision research but rarely attempted since the resources required to design custom hardware are usually not available. Instead researchers direct their efforts toward devising vision algorithms that are efficient when implemented using standard processors. They thus avoid due to computational complexity approaches which are not feasible in software but might work well in hardware.

Another option not widely known in the vision community to employ programmable hardware as the implementation vehicle. Programmable hardware has already been shown to be a good solution for many signal processing tasks that are similar to machine vision [25][26][27][28], and using a programmable system reduces the time, cost, and expertise required to create a working hardware prototype. It reduces cost by avoiding the enormous expense of chip and board fabrication and by spreading the cost of the system over all of the vision and non-vision applications for which it might be used. It reduces time and expertise requirements by permitting less rigorous design and testing. When using programmable hardware, the cost of fixing a bug after design is the minimal penalty of recompiling rather than the enormous expense of refabricating. The cost of a design change is similarly reduced, thus allowing much more experimentation using differing hardware implementations.

The goal of this research is to explore the feasibility of programmable hardware as a platform for complex real-time machine vision. We will do this by implementing a complex vision task on the Transmogrifier-2a (TM-2a), a large configurable hardware system [18][19]. The vision problem we will focus on is *object detection*: the task of locating an object in an image despite considerable variation in lighting, background and object appearance. Object detection is one of the best-known and most useful machine vision applications, and is also difficult and computationally complex. The specific case we will consider is face detection, motivated because face analysis is a very active area of vision research. Face analysis can be used in security applications, telecommunications, human-computer interfaces, entertainment, and database retrieval. In order to analyze a face in detail, however, the face must first be located. Many face analysis algorithms are developed with the assumption of controlled environments in which face detection is trivial. Such assumptions become invalid as the applications move into uncontrolled environments, so accurate face detection is necessary. Since detection is only a first step before recognition and other tasks, it needs to be done quickly.

The first stage of this research was to develop an object detection strategy that would be accurate, efficient in hardware, and applicable to faces. The literature proposes a considerable variety of approaches, but the best of these are either inherently serial or require too much hardware to implement. We have developed an object detection framework aimed at a hardware implementation and based on a new machine learning method. The second stage was the adaptation of the framework for the specific problem of face detection. The third and final stage was to implement the method on a programmable hardware system. The final implementation runs at 30 frames per second and detects faces over three octaves of scale variation. This is approximately 1000 times faster than the same algorithm running in software on a 500MHz UltraSparc and approximately 90 to 6000 times faster than the reported speed of other software algorithms.

This dissertation begins by presenting background in Chapter 2. Chapter 3 presents the object detection framework, and Chapter 4 discusses its use for face detection. Chapter 5 describes the implementation of the face detection algorithm in programmable hardware. Finally, Chapter 6 presents conclusions and future work.

Chapter 2

Background

This thesis has two goals: to develop a face detection method that is both accurate and efficient in programmable hardware; and to implement this algorithm on a large programmable system. In this chapter, Section 2.1 first reviews the face detection problem and presents a general face detection approach. Sections 2.2 and 2.3 then consider in detail two stages of this general approach: image processing and pattern classification, respectively. Section 2.4 looks at programmable logic and programmable hardware systems, and Section 2.5 reviews how these have been used to perform tasks similar to the one at hand.

2.1 Overview of Face Detection

2.1.1 Problem Definition

For this thesis, face detection is defined as the problem of locating faces in an image in the presence of uncontrolled backgrounds and lighting, unrestricted range of facial expression, and typical variations in hair style, facial hair, glasses, and other adornments. These variations must be handled by any face detection method which hopes to operate in an uncontrolled environment. We do not assume the presence of colour information, motion information, or other parts of the body, since the human vision system proves that it is possible to detect faces without them, and they would introduce additional potential failure modes for the system.

2.1.2 Face Detection as Object Detection

The problem of face detection falls into the much larger category of object detection. Although the terms “detection” and “recognition” are often used interchangeably in the literature, we define them as follows: given one or more object classes, “detection” is the task of distinguishing members of one class from members of another, and “recognition” is the task of distinguishing between members of the same class. The ambiguity between these two problems comes from the fact that whether one is doing detection or recognition depends entirely on how one defines the object class-es.

In the most typical detection problem there are only two classes: the class of target objects (fac-es, for example) and the class of all other objects, or the background class. Any object detection problem that fits this model is then uniquely defined by two factors: the variation in the target ob-ject's appearance; and the variation in the appearance of all of the non-target objects. If either of these kinds of variation is not present, accurate detection becomes trivial. If the target objects ap-pear against an unvarying background then detection consists of a simple subtraction operation, even if the object itself varies wildly in appearance. If the target objects have a precise, unvarying visual appearance then detection can be performed by a matched filter even in nearly arbitrary clut-ter. In the most interesting detection problems there is significant variation in both the appearance of the target objects and the appearance of the background, such that there exist instances of each class that are indistinguishable from instances of the other.

Face detection is one of these problems. Faces can change drastically in visual appearance from one individual to the next and even for a single individual over the space of expression, facial hair, and adornments such as glasses. Due to their 3-dimensional structure, the appearance of faces also depends greatly on lighting conditions. As for backgrounds, they are essentially arbitrary; when one considers the space of likely surrounding objects, both natural and man-made, we are able to exclude from possibility only the most unnatural kinds of artificially generated noise.

One source of target appearance variation that is common to all visual detection problems is object pose. The three types of pose variation are illustrated in Figure 1. Objects can vary in size depending on their distance from the camera, and they can be rotated through three degrees of free-dom. Changes in size and rotation in the camera's image plane pose only a computational problem as in any case the image could be scaled or rotated to correct for them. Rotation in depth poses a much more serious problem as the resulting appearance depends on the three-dimensional structure of the object. One useful way to categorize detection methods is by the extent to which they can tolerate variation in the different components of object pose, and we will consider this when we

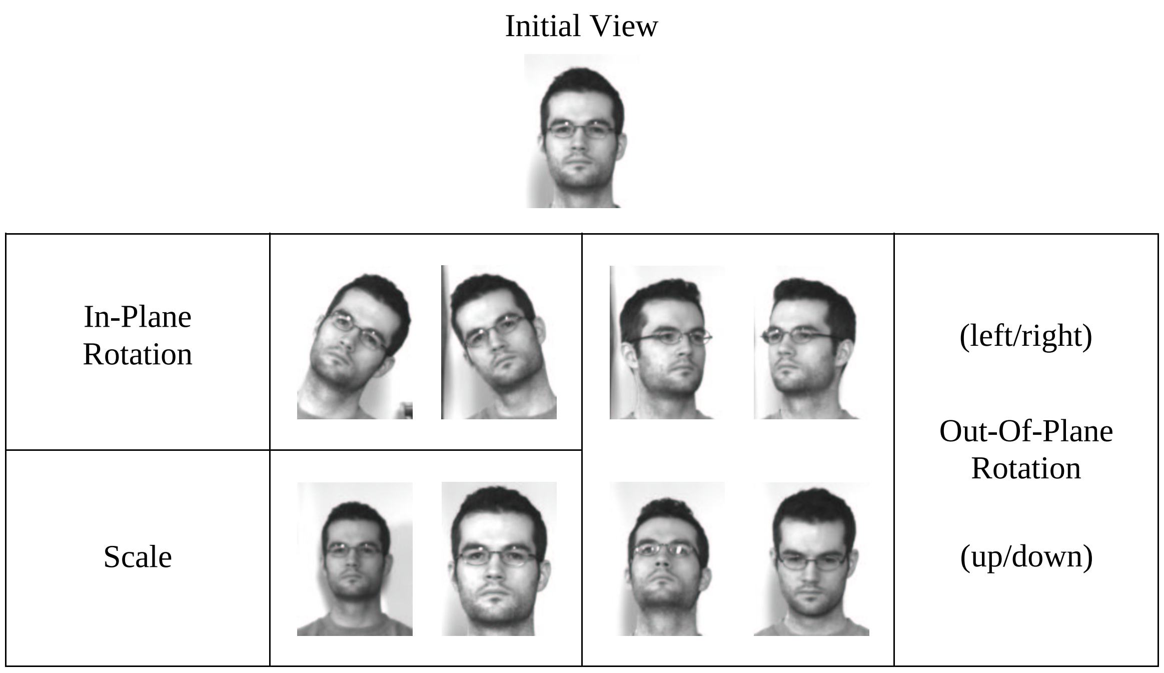

Figure 1: Object Pose Variation

look at previous work in face detection in Section 2.3.2 below.

2.1.3 General Approach to Face Detection

The field of face detection is characterized by a very broad range of approaches, so it is difficult to present an accurate general case in significant detail. Most systems, however, proceed in three stages. The first stage transforms the input image in some way that extracts or emphasizes important information and thus improves detection accuracy. This stage is called *image processing*. The second stage selects appropriate portions of the transformed image to evaluate further. This stage is called *image search*. The third and final stage evaluates the output of the first two stages and classifies it as target or background, face or non-face, and is called *pattern classification*. Figure 2 illustrates these stages.

It is important to understand that there are plenty of exceptions in practice to this simple model. Image processing and image search may be reversed, combined, or interleaved in multiple stages. Many applications have no separate image processing stage at all. Regardless, considering this general approach provides a good introduction to the basic tasks involved in face detection. Below we briefly describe the stages and their role in the system as a whole. Following sections examine image processing and pattern classification in more detail.

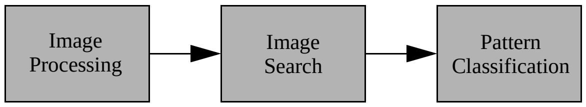

Figure 2: Face Detection Stages

Any given face detection system could use a considerable variety of image processing tasks, as the particular ones chosen will depend on the requirements of the pattern classification stage. The processing stage must extract information that the classification stage needs and suppress variation that the classification stage cannot handle. Two common tasks are lighting correction and filtering. Lighting correction reduces the effects of variable lighting intensity and direction, and filtering extracts information at particular spatial frequencies and orientations. Section 2.2 below discusses image processing.

The image search method chosen also depends on the capabilities of the pattern classification stage. One very simple and common method is to systematically select every possible sub-image from the input, potentially including scaled and/or rotated sub-images in order to compensate for face size and in-plane rotation. This is often used for fixed-size face “templates”. The approach is computationally expensive, however, and so recent work has focussed on developing ways to reduce the search space. In some cases, additional information such as colour or motion is used to find portions of the image which are likely to contain a face. In other cases, the classification step is designed to either be inherently invariant with respect to scale or rotation, or designed to provide a method of directed image search.

Pattern classification is the most critical and complex of the three stages. The accuracy of the face detection system relies primarily on the performance of this stage, and faces, as we discussed above, are particularly difficult to classify because of the amount of possible variation in both face appearance and background appearance. Section 2.3 below discusses pattern classification.

2.2 Image Processing

The first stage in our general face detection model is image processing. This stage must transform the incoming data such that it is suitable for use by pattern classification. One common image processing tool, image filtering, is an important stage in many vision systems because it emphasizes certain types of information in an image and suppresses others. In this thesis we use a specific pair of filters called G2 and H2 [16]. Below we give an overview of the image filtering process and then describe the properties of these filters in detail.

2.2.1 Image Filtering

There are many types of filters and many kinds of image data on which they operate, but we are only going to consider one case: linear FIR filters operating on greyscale images. An FIR image filter consists of a two-dimensional array of coefficients sampled from the filter's continuous impulse response. This is often called the filter kernel. The filter output for an image is generated by performing a 2-D convolution operation between the image and this kernel. One useful way to visualize the filtering process is to imagine the kernel sliding across the image surface such that it is centered, in turn, over each pixel location in the image. At each location each kernel coefficient is multiplied with the greyscale value directly underneath it. The filter result for that location is the sum of these products. Those familiar with 1-D FIR filtering or convolution will recognize this as a simple extension to two dimensions.

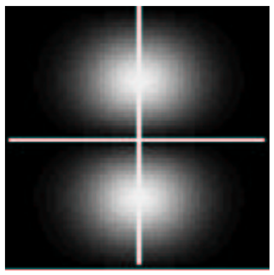
Figure 3: Frequency Response of a Vertical Bandpass Filter [16]

A 2-D filter has a 2-D frequency response. Figure 3 shows the frequency response of an FIR band-pass filter. The pass-band of the filter is defined by both a spatial frequency range and an orientation range. This particular filter only responds to signals in the image that have a roughly vertical orientation. Indeed, the majority of image filters are orientation-selective; while it is possible to construct filters that respond to a given frequency at any orientation, the orientation information is then lost. To avoid this and still capture all of the necessary structure, vision applications often apply several rotated versions of an orientation-selective filter.

Figure 4 shows a standard graphical representation of the kernel coefficients for a set of band-pass filters. For purposes of display the coefficient values have been scaled to fit into an unsigned 8-bit representation, producing a standard greyscale image. Dark areas in the picture are negative coefficients, light areas are positive coefficients, and neutral grey areas are at or close to zero. Images such as this are commonly used in machine vision and image processing papers to give the reader an immediately understandable representation of the structure of a filter.

2.2.2 G2/H2 Properties

G2 and H2 are members of a class of filters useful for a range of machine vision tasks [16][17]. Figure 4 shows the kernels of the 0 and 90 degree orientations of both G2 and H2. G2 is the second derivative of a Gaussian, and H2 is the Hilbert transform of G2. For the purposes of this work, they have three important features: they are band-pass filters that form a quadrature pair and are thus useful tools for multi-scale texture analysis; they are X-Y separable, which makes them efficient to implement; and they are orientation-steerable, which allows us to generate a version of the filters at any orientation using a fixed set of basis filters.

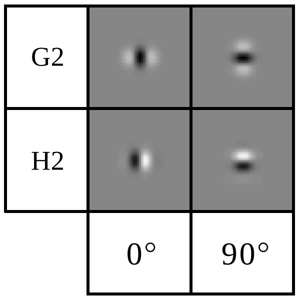

Figure 4: G2/H2 Filters at 0 and 90 Degrees

An X-Y separable filter has an impulse response that may be expressed as a product of two functions: one which depends only on X, and one which depends only on Y. Consider a the separable filter with kernel $K[x][y]$ defined as:

$$K[x][y] = F[x] \bullet G[y] \tag{EQ 1}$$

If we convolve $K[x][y]$ with the image $I[x][y]$ to produce the filter output $O[x][y]$, we can separate the convolution into separate X and Y stages:

$$O[x][y] = \sum_{v=-(N/2)}^{N/2} G[v] \bullet \left(\sum_{u=-(N/2)}^{N/2} F[u] \bullet I[x+u][y+v] \right) \tag{EQ 2}$$

where N is the size of the filter kernel. The image is first convolved with a row vector of X coefficients, and then these X results are convolved with a column vector of Y coefficients. This reduces the filtering process from an $O(N^2)$ operation to an $O(2N)$ operation.

The other important property of G2/H2 is orientation-steerability. An orientation-steerable filter is one that can be generated at any orientation using linear combinations of a finite set of basis filters. For G2, three basis filters are required; for H2, four are required. This property contributes further to the pair’s efficiency, because it restricts the number of unique filter kernels convolved with the image to seven, regardless of the number of distinct filter orientations the application needs. If we only needed one or two orientations, however, we would probably not bother to use this property as the cost of applying all of the basis filters would exceed the cost of directly applying the oriented filter versions.

2.3 Pattern Classification

The final stage in our general face detection system is pattern classification. Pattern classification takes as input an image region enhanced by the processing stage and selected by the search stage. As output it produces a decision as to whether the region represents a face or represents background. All face detection methods must use some form of pattern classification to distinguish faces from background, and the accuracy of this classification is the most important contributor to the overall accuracy of the system. When designing a face detection system, it is therefore critical to design an accurate pattern classification method. In this section we first discuss one of the most powerful techniques for constructing accurate classifiers: machine learning. We then review classification methods used in previous work and analyze their performance. Finally, we present the machine learning method on which the classifier used in this work is based.

2.3.1 Machine Learning

Face detection is a difficult task because of the variation present in both face and background appearance. Given the complexity of the problem, it is difficult to hand-craft a solution that will have satisfactory accuracy. Instead, one of the best ways to build a classifier is to collect a large set of classification examples, create a parameterized classification function, and then have a computer optimize the function parameters such that the output better agrees with the examples. This process is called *machine learning*. Machine learning methods approximate the underlying statistical properties of an unknown system by observing the system's behaviour. The unknown system is represented by a parameterized *model*, and it's behaviour is captured in a set of samples called a *training set*. An optimization algorithm modifies, or "trains", the model parameters such that the error between the model's predictions and the training set data is minimized.

In the absence of machine learning, application designers must rely on their own domain knowledge to create an approximation of an unknown system. This process is highly susceptible to the often incomplete and inaccurate nature of human memory and reasoning. If the system is very complex, accurately hand-crafting an approximation may not be possible at all. In contrast, a machine learning method has only those biases explicitly included in the model and optimization procedure. Even for very complex systems machine learning provides a directed means to search the space of model parameters and provide a result that fits the examples given and generalizes to new ones.

Many machine vision applications use machine learning concepts. An image of a scene is a very under-constrained description of that scene's contents, and thus machine vision techniques must be given a good deal of prior knowledge about the structures they are looking for in order to extract any information at all from the data. Machine learning techniques allow this prior knowledge to be captured from examples of the structures rather than explicitly stated. The most accurate face detection techniques are those which make consistent use of machine learning, as we discuss in Section 2.3.2 below.

In this section we first review the major styles of machine learning, which we divide into supervised and unsupervised methods. We then describe general machine learning issues around choice of model, model training, and model testing.

Styles of Learning

There are two major styles of machine learning: supervised and unsupervised. Both styles have been used in the face detection systems we will discuss, and the learning method used in this work combines elements of both. It is important to understand the different goals and characteristics of each type to evaluate how choosing one or the other can affect the performance of a face detection system.

Supervised learning refers to methods in which each training example has two sets of values: a set of known inputs and a set of target outputs. The goal of training is to have the model produce the correct outputs when presented with particular inputs. These methods are given the label "supervised" by analogy to a human learning process in which the learner is monitored and corrected at each step. This category includes the most widely known and used learning techniques, ranging from polynomial fitting to artificial neural networks.

While supervised learning approximates input/output relationships, unsupervised learning approximates generative processes. Given a training set of patterns from a single target class, the goal of unsupervised learning is to learn a model of the statistical structure of the patterns. Once trained, such models are often used to calculate the probability that a new pattern belongs to the target class, to encode and then reconstruct patterns, or to generate completely new example patterns that conform to the learned statistics. These methods are labeled "unsupervised" since no explicit target output values are given, but it is important not to take this label at its semantic face value. In a very real sense the data themselves are both the known input and the target output, as many unsupervised learning methods measure their performance by coding an example, reconstructing it, and then comparing the reconstruction with the original. In order for these methods to work, human intervention is still required to ensure that the training set contains only positive examples of the target class.

Unsupervised learning methods are generally less well-known than supervised methods, but they have proven to be very powerful and useful tools. The basic idea behind unsupervised learning can be summarized as “representation equals analysis”: if we try to learn ways to accurately and efficiently represent the target patterns, we are likely to end up discovering interesting structure about those patterns. This emphasis on representation and reconstruction makes unsupervised learning excellent for problems such as efficient domain-specific video or sound coding techniques. Unfortunately, it is not so well suited to detection problems. When performing detection, we are interested in what differentiates our target pattern from other non-target patterns that are likely to occur. Unsupervised learning only analyses the target pattern with the goal of representing it, and the details that are useful for accurate representation are not always or even usually the details that are useful for detection.

Models, Training, and Testing

Even with the wide variety of approaches to machine learning, there are three steps that most application designers perform: choose a model architecture; train the model; and test the performance of the trained system. Although the details of these steps vary considerably from method to method, there are general guidelines and theory on how to perform them so as to encourage good performance and ensure accurate measurement of that performance. In this section we discuss typical ways of approaching these tasks.

Many machine learning methods require the designer to choose a specific model architecture. It is important to choose an architecture with an appropriate level of complexity and an appropriate internal structure. The complexity of a model is determined largely by the number of free parameters, and the greater the number of model parameters, the greater representational power the model has. If a model is too simple it will not be able to capture the underlying structure of the target system and will perform badly. For example, a linear model could never fit quadratic data accurately. This is called *bias error*. If the model is too complex it will be under-constrained by the training set and will over-fit it, causing poor performance on new data. For example a, 9th-order polynomial fits any set of 10 training points precisely, including any noise in the data. This is called *variance error*. Closely related to the issue of choosing model complexity is that of choosing model structure. With many learning techniques the designer has the opportunity to impose certain structural constraints on the model. Doing so reduces the number of model parameters by removing those which would have allowed the model to move away from the imposed structure. If the structure is guided by knowledge about the target system, however, we can reduce the number of model parameters without reducing the effectiveness of the model; we reduce the variance error without adding bias error. Choosing model structure is something of an art because of this. Although human domain knowledge is problematic when it comes to manually defining the gritty details of an approximation, it is typically the best way to craft a model structure to learn those details. Even so it remains a good idea to mitigate the designer's biases by training a set of models with different structures and complexity, and either keeping the best one or combining their results in some fashion.

Once a model is chosen the next step is to train it, and the most important component of training is the training set. When it comes to training sets, one can rarely have enough data. Having a large number of samples is one of the best ways to ensure good results. Sheer number of examples, however, is not the only consideration. Ensuring that the training set covers a broad variety of operating circumstances is also vital. The learning algorithm will find whatever statistical relationships exist in the data, even the ones that occur by accident, and it will not find those relationships which do not exist in the data. There are many cases of machine learning systems that were trained on data that had strong spurious correlations and thus performed in very strange ways once deployed. As an example, consider what might happen if a face detection algorithm were trained with a set of face images taken with the subjects standing against a brick wall. The trained model might include more information about the structure of the wall than about the structure of the faces. In operation it might do a great job of detecting brick walls, but be utterly unable to find a single face.

In practice, it is almost never possible to achieve either the number or variety of training set examples required to avoid over-fitting altogether. To address this problem, machine vision researchers have developed the concept of regularization. Regularization places soft *a priori* constraints on parameter values during training that encourage the model as a whole to prefer simpler solutions over more complex ones. These constraints are set to be weak enough that the major relationships in the data are learned and strong enough that the occasional spurious correlations are smoothed away.

Finally, we need to be able to estimate the performance of the trained system on new data. For this purpose we use a test set, which is a set of data not included in training but only used to determine the accuracy of the system. Typically the designer will randomly select 10% of the available examples and reserve them for the test set, leaving the remaining 90% for training. Training is repeated several times with different randomly selected test and training sets and the results are averaged. This ensures that the measured accuracy is not influenced by the unlucky choice of a test set that is not representative of the data as a whole.

2.3.2 Previous Pattern Classification Methods

In this section we review and discuss a number of recent approaches to pattern classification in face detection. At the beginning of this chapter we gave a definition of the specific face detection problem considered in this work. Even with this limiting definition, however, there are a large number of differing approaches in prior work to examine and compare. To reduce this number, we will only consider *appearance-based* approaches: those that model a face as one or more two-dimensional patterns and do not have an explicit three-dimensional description of head or face structure. Viewed as two-dimensional patterns of intensity variation, faces are objects with distinct subpatterns that occur over scopes ranging from highly local to nearly global. Over the space of identity, expression, lighting, and pose these patterns can deform and move independently with respect to one another.

The key to accurate face detection is to identify those patterns which are stable over the space of face appearance and are useful for distinguishing faces from background, and then to unify these patterns in a flexible manner into a whole face detector. As we review previous face detection classifiers, we will be considering in particular how each is biased towards particular types and scopes of patterns, how each determines which patterns to use, and how these patterns are connected. At the end of the section we will summarize and synthesize the prior work and use this analysis as the basis for developing a robust face detection method.

The simplest appearance-based face detection method is perhaps the matched filter or correlation template. The template consists of a single, properly normalized (for statistical purposes) image of a face. The template is created by averaging a training set of face images, which is a very simple type of unsupervised learning. This kind of method does not typically perform well for the simple reason that a single fixed template is too inflexible to capture enough appearance variation.

A single template represents all face patterns from local to global with a single mean case, and represents them together in a rigid spatial arrangement. Even if the training images are normalized for position and scale with respect to some facial landmarks, independent movement or deformation of patterns associated with other landmarks will result in a blurring effect after averaging. Patterns with global scope tend to be affected little by this, while very local patterns may be entirely obscured, so such methods favour global patterns.

There have been a number of methods which improve on the basic correlation template by dividing the face into separate local regions and using more complex learning methods to capture greater variation. Mogghadam and Pentland [6] use four regions corresponding to four facial landmarks: left eye, right eye, nose, and mouth. They use an unsupervised learning technique called Principal Components Analysis (PCA) to model the variation in these features. PCA generates a mapping from the high-dimensional input pixel space to a lower-dimensional feature-specific space. Once PCA has determined this mapping, two measures are used to decide whether a particular sub-image matches a feature: a measure of how much of the information in the image is lost by the mapping; and a measure of how likely it is that the mapped point corresponds to a valid feature. These probabilistic measures are determined by another unsupervised learning stage. A third unsupervised learning stage models the spatial relationships between the four features. On a very simple test set with little variation, this method detects 90% of the faces. One of the major drawbacks of this approach is that no attempt is made to model and account for close non-face patterns: PCA finds a mapping which is optimal for face representation but which may not be useful for classification. Lew [4] addresses this problem by using a very similar method with two major differences. First, a supervised learning stage analyses face and non-face images and determines which pixels are the most important for distinguishing faces from background. Second, the authors use a supervised learning method which is similar to PCA, but which finds a mapping directed towards classification.

The methods discussed above have solved the correlation template's problem of representing local and global patterns together in a single template by splitting that template into a set of smaller ones that can vary independently. While doing so improves the flexibility of the model, it also ignores a considerable amount of information. These methods place absolute limits on pattern scope; patterns which would extend beyond the size of any single smaller template can no longer even be represented. They also require a choice of which sub-patterns to pay attention to; while a single whole-face template can at least attempt to represent all face patterns, a set of local templates cannot represent any pattern that falls outside of the chosen sub-regions. This choice of pattern is made manually, and so is subject to all of the inaccuracies of human reasoning.

Leung *et. al.* [14] illustrates an extreme case of sacrificing information for flexibility. They use a face model consisting of local pattern detectors connected via a complex shape model. The patterns and shape model are invariant with respect to in-plane rotation and scale, and are also very tolerant with respect to out-of-plane rotation. The resulting model can predict the positions of missing features during search and evaluate the quality of a face candidate by calculating its probability under the model parameters. The authors chose a multi-orientation, multi-scale set of derivative-of-Gaussian filters to describe 12 facial landmarks. The responses of a given landmark to these filters are assembled into a vector that serves as a landmark template. At run time the same filters are convolved with the input image producing a similar vector at each location. These vectors are compared with the feature vectors to determine where the local patterns are present. The individual landmark detectors are, however, fairly unreliable. Each generates a large number of false positives. The authors use their shape model to look for groupings of multiple local features that conform to the expected arrangement

While this method inherently deals well with variation due to face pose, it does not deal well with variation due to other factors such as identity and expression; the authors report a detection accuracy of only 70%. The likely reason is that the small number of very local features do not take enough information into account, so that faces that happen to vary considerably in those particular areas cannot be detected. While the local pattern vectors and the spatial relationship model are trained using unsupervised learning, the choice of facial landmarks is manual and thus arbitrary. Part of the degradation in performance could be due to using landmarks that are not truly stable indications of the presence of a face. This stability can only be judged reliably by a rigorous statistical learning method.

The most successful techniques find ways to balance local and global scopes and balance information versus flexibility. The key to doing this well is to use machine learning to decide what information is truly important. To this end Rowley *et al.* [10][11] propose a neural network face detection system. The system has a 20x20 pixel receptive field which is applied at every location in the input image. The network is structured to allow for both a small set of large patterns and larger set of local patterns. The candidate sub-image is passed into this detector network, which is trained to produce a “1” on its output if the area contains a face, and a “-1” otherwise. One problem associated with training a face detection network using supervised learning is that it is difficult to manually choose challenging non-face examples, as one never knows beforehand what cases the network will classify badly. To overcome this problem the authors use a “bootstrap” training method; areas which are incorrectly identified as faces are included more often in subsequent training. The final system arbitrates between a redundant pair of independently trained networks to produce greater accuracy. Several different network architectures and arbitration schemes were used producing differing levels of accuracy, but in general the detection rate was 85% to 90% with few false positives. The good performance of the system and the widespread acceptance and understanding of neural networks have made this method popular. McKenna *et. al.* [9] use the detector net from [10] as a verification stage in their motion-based face detection system. Han *et. al.* [5] also use the detector as a verification stage. The major limitation of this approach is the hand-crafted structure of the network; while it is useful and intuitive, it also places hard limits on the sort and arrangement of information the network can use.

Schniederman [12] uses a very different modelling technique and produces better results still. The face is modelled by a discrete set of patterns combined at different positions and over three different scales. The likelihood of a particular pattern type occurring at any given position and scale is calculated for both faces and non-faces, and this information is used during run-time to classify candidate image regions. The multi-scale nature of the model allows a considerable range of pattern scopes to be accounted for, and the explicit comparison with non-face distributions causes patterns with little discriminatory power to be ignored. Using the same test set as Rowley *et al.*, this system produces a 10% better detection rate given the same number of false positives.

Discussion

From our review of pertinent current methods, we can see some general approaches that work well. A robust face detection method is able to accurately account for patterns with varying scope, from local to global. This typically involves breaking up the face into a set of independent patterns and allowing these patterns to move in relation to one another. As much as is possible, the scope, location, and arrangement of these patterns is learned rather than chosen manually, and the learning process focusses on discriminating between faces and non-faces rather than on attempting to accurately represent face images alone. Once the useful patterns have been identified they have to be flexibly integrated into a whole face detector, either implicitly as in multi-layer neural networks or explicitly via statistical models of pattern position.

The methods we reviewed each satisfied these goals to different degrees and in different ways. One thing that is common to nearly all, however, is that the designers needed to assemble a hodge-podge of techniques: shape statistics, Gaussian clustering, neural networks, supervised learning, unsupervised learning, and large contributions of manual construction. There are two examples in which this mixing of techniques is most obvious. The first is the selection of pattern locations and scopes. In all of the methods we reviewed there is a significant amount of designer choice required in determining the possible location and scope of patterns used, if not required in determining the patterns themselves. Even in Rowley *et al.* [10] the network architecture allowed only three different pattern scopes and a distinct set of positions, and this is also true of Schniederman [12]. The second example is the separation between the detection methods used to find individual patterns and the unification methods used to find a characteristic arrangement of the patterns. In all but Rowley *et al.* [10] the method used to detect pattern arrangements had no relationship to the method used to detect the patterns themselves.

We have discussed at several points why designers should avoid inserting arbitrary decisions into their systems, but have not touched on any benefits of using a single learning method rather than a combination of methods. What we would ideally like is for both the task of learning a characteristic arrangement of patterns and the task of learning the patterns themselves to be expressed in a single theoretical framework. There are two major benefits of this: elegance and extensibility. Elegance is a badly defined term, but we would consider an elegant solution to be one which accounts for the required complexity within a rigorous framework and without significant special case requirements. This is of greatest importance during design as it avoids ad-hoc solutions to parts of the problem that are otherwise not handled. Extensibility comes as a result of considering the unification stage to be an additional detection stage in which we look for patterns in the outputs of the initial pattern detectors. We can learn patterns in these outputs exactly the same way as we learn patterns in the input by simply repeating an identical second stage of analysis on top of the first. In the same way as we looked for different scales and types of patterns in the input, we now look for them again in the pattern detection results. Once we are able to perform this analysis “stacking”, we can repeat it as many times as required by the structure of the data. The standard ANN is a good example of a learning method that displays these properties; neurons in the first layer are sensitive to certain patterns in the input, neurons in the second layer are sensitive to certain patterns in the first layer, and so on. Each neuron, regardless of where it is located, is trained and activated in precisely the same manner as any other neuron. This has proven to be a very elegant, extensible, and useful method indeed. The major difficulty with ANNs from our perspective is that the designer must manually craft a network architecture, thus limiting the types of patterns the net can use.

Any single method that is going to satisfy these requirements will have to be able to perform two tasks automatically: *decompose* the input into an appropriate set of stable, characteristic patterns; and build an appropriate *hierarchy* of pattern detectors by applying this decomposition at more than one level of analysis. In the next section we discuss the CFA algorithm we use in our own face detection application and which was developed to perform this sort of analysis.

2.3.3 Competitive Feature Analysis (CFA)

In the previous section we reviewed some past and current face detection methods in order to evaluate what strategies were the most successful and why. We found that the best methods used machine learning techniques to discover the important patterns in the input and to model how these patterns are arranged. All of the existing approaches, however, need significant human intervention to limit the scope and position of potential patterns, and all save one use completely different methods to learn the patterns and then learn their spatial arrangement. In the conclusion, we noted that what was needed was a method that could perform both automatic decomposition, to find important patterns, and automatic hierarchy building, to unify them.

This section describes the Competitive Feature Analysis (CFA) learning method. CFA was developed at the beginning of this work with visual object detection specifically in mind, although it is not considered part of this thesis and will be developed in future research. Presented with a training set of object images, CFA is designed to decompose the object into characteristic sub-patterns through the use of competing pattern detectors called *features*. Each feature is responsible for a particular pattern present in the object's appearance, and the features compete with each other to be responsible for larger portions of the object. Features have nonlinear outputs which may be used as inputs to higher-level features in a hierarchy, providing an elegant method of pattern unification. The competitive learning algorithm strongly couples representation with detection and provides an elegant way to integrate non-target examples. This approach ensures that the patterns learned are both stable and characteristic of the target class.

We first discuss the particular type of inputs required by features and examine how a feature internally represents the pattern for which it is responsible. Next we show how this representation is used to produce a detection probability given input, and also how it is used to reconstruct input given a detection probability. This is followed by a discussion of the competitive learning algorithm. We briefly look at feature hierarchies, and finally summarize the properties of the CFA method. In order to avoid unnecessary detail in this section only simplified versions of the most important CFA formulas are shown. Appendix A contains the full formulation for those interested.

Feature Inputs

One unusual aspect of CFA features is the type of inputs they use. CFA has a probabilistic formulation, and as part of this formulation it requires that feature inputs are in the form of probabilities. This is different from most other learning methods, which can typically operate on any real-valued input. It also seems problematic for visual detection, as greyscale images are expressed as real-valued pixels, not probabilities.

To evaluate the implications of this input requirement, it is instructive to review some basic probability theory. Any probability specifies the likelihood of a random event, and this random event is defined as the occurence of a random variable meeting certain criteria. CFA requires that the variables associated with feature inputs are *discrete*, meaning that each can only take on a set of mutually exclusive states. These states constitute the sample space of the random variable. A good example of a discrete random variable is the typical speed switch on a fan, which might have the settings “off”, “low”, and “high”. The switch cannot take on values between these states, and it must always be in one state or another. The current state of the fan switch can be represented by a set of probabilities. For example, the set {0.1, 0.6, 0.3} indicates that there is a 10% chance that the switch is “off”, a 60% chance that it is on “low”, and a 30% chance that is on “high”. Since the switch is always in one of these states, the probabilities in the set must sum to one

The state of an input to a CFA feature is similary represented by a probability set. The practical result of this requirement is that the designer of a CFA-based detection application must determine beforehand a discrete representation for the pixel data, that makes sense in the context of the application. The image processing stage of the application will then be responsible for transforming the image into this representation. One possible choice would be to represent a pixel as one of two states: either less than or not less than a certain greyscale threshold. The associated transformation would then simply covert each pixel to one bit by comparing its value to the threshold. The inputs to a CFA feature in this case could only be either {1.0, 0} or {0, 1.0}, since each pixel is either completely below the threshold or not. A more complex method that assumed a gaussian noise distribution on the pixel values would have probabilities other than 1.0 and 0, with a pixel exactly equal to the threshold perhaps having the probabilities $\{0.5, 0.5\}$. This simple representation would likely be very sensitive to lighting changes, but it provides a useful example.

Pattern Representation

Each feature in a CFA object model has an internal representation of some pattern in that object's appearance. This pattern is expressed as a prediction of the state of each input, and the predictions have the same format as the inputs: a set of state probabilities. Continuing our pixel thresholding example from the previous section, a feature might represent its prediction for two of the inputs in its pattern as $\{0.9, 0.1\}$ and $\{0.3, 0.7\}$. The first pixel is strongly predicted to be below the threshold. The second pixel is predicted to be above the threshold, although with less certainty. An important aspect of this model from a probabilistic perspective is that the inputs are assumed to be independent of one another; if the value of one input is were known, this information would not affect the prediction for the other input.

The pattern model described above is one of two models contained in a CFA feature. Since the ultimate task of a feature is to detect its pattern, it also contains a model of what appears at its inputs when its pattern is not present. This second model is called the *background* model, and it is expressed in exactly the same way as the first.

Finally, each feature keeps track of one additional value: the likelihood that it's pattern will be present in any given image. Since this probability represents a best detection guess prior to even seeing the input, it is referred to as the *a priori* probability that the feature's pattern is present.

Input Responsibilities

CFA, as its name states, is a competitive learning method. During training, CFA features compete with each other to detect patterns in the target object's appearance. To indicate how well a feature is performing on different portions of the object, it has a value associated with each of its inputs that determines its *responsibility* for that input. The responsibility value is in the range [0, 1] and acts as a weighting factor during detection and learning. As is shown in the discussion of competitive learning below, the features with the most accurate models of object patterns will receive greater responsibility for those patterns as training progresses.

Pattern Detection

In this section we look at the activation function of a feature and show how its pattern model, background model, and responsibilities are used to perform pattern detection. The current state probabilities for each input are compared with both models, and this comparison is used to calculate the feature's output, which is the probability its pattern is present. If the pattern is present in the image, we will say that the feature is also 'present'.

The formulas for calculating the output are given below, where

- o_k is the output of feature k
- a_k is the activation of feature k
- a_{kn} is the partial activation of feature k associated with input n
- N_I is the number of inputs
- N_S is the number of input states
- i_{ns} is the input probability that input n is in state s
- p^+_{kns} is the probability assigned by feature k to the event of input n being in state s given that feature k is present
- p^-_{kns} is the probability assigned by feature k to the event of input n being in state s given that feature k is not present
- r_{kn} is the responsibility of feature k for input n
- p^+_k is the *a priori* probability that feature k is present
- $(1 - p^+_k)$ is the *a priori* probability that feature k is not present

$$a_{kn} = \sum_{s=0}^{N_S - 1} i_{ns} \ln\left(\frac{p^+_{kns}}{p^-_{kns}}\right) \qquad \text{(EQ 3)}$$

$$a_k = b_k + \sum_{n=0}^{N_I - 1} r_{kn} a_{kn} \tag{EQ 4}$$

$$b_k = \ln\left(\frac{p_k^+}{1 - p_k^+}\right) \tag{EQ 5}$$

$$o_k = \frac{1}{1 + e^{-a_k}} \tag{EQ 6}$$

Let's look first at (EQ 3), which calculates the contribution a_{kn} of a single input n to the overall activation a_k of feature k. The feature has two sets of probabilities for each input: p_{kns}^+ and p_{kns}^-. The first set is its prediction for the input given that the feature is present. The second set is its prediction for that input given that the feature is not present. The contribution of a particular input to the overall activation is a function of that input's probability under these two different predictions. To compare the probabilities CFA uses a cross-entropy error function, a standard formula for comparing probability distributions. If p_{kns}^+ is greater than p_{kns}^- then a large i_{ns} will make a positive contribution to the activation. If the reverse is true, then a large i_{ns} will make a negative contribution. If $p_{kns}^+ = p_{kns}^-$ then the value of i_{ns} has no effect on the activation. The interpretation of this last observation is that if input n being in state s has the same predicted likelihood regardless of whether the feature is present or not, then the actual input likelihood gives us no information.

If we move to (EQ 4), we see the other parameter that controls how much a particular input contributes to the overall feature result: the responsibility, r_{kn}. As r_{kn} increases, input n has a greater effect on the activation of feature k; as r_{kn} decreases, input n has less effect. Inserting r_{kn} into the formulation is critical to competitive learning, as we show in the next section.

Once all of the input contributions have been summed there is another term, b_k, added to the result. This is the feature's bias, and in (EQ 5) we see it is the natural log of the ratio of two probabilities, p_k^+ and $(1 - p_k^+)$. p_k^+ is the *a priori* probability that feature k is present, and thus $(1 - p_k^+)$ is the probability that it is not present. b_k is called the bias because it introduces an additive term into the activation which represents the features expectation before it is even shown the input. If p_k^+ is greater than 0.5, then this term will be positive; if it is less, this term will be negative. If it is equally likely that the feature is present or not present, then the bias will be zero.

The activation a_k has a possible range from negative infinity to positive infinity. We need to use this value to generate a probability between zero and one. Given our derivation so far, the meaningful way to do this, in a probabilistic sense, is to use the sigmoid activation function given in (EQ 6).

Input Reconstruction and Competitive Learning

During learning, the current CFA model is iteratively presented with an image from the training set and then adjusted to better account for the image contents. Each of these iterations has two stages: a detection stage, which was discussed above, and a reconstruction and learning stage. During the detection stage all of the features calculate their outputs. The resulting ensemble of feature outputs can be viewed as a coding of the input image in terms of the patterns it contains. To determine how accurate this coding is, it is used as the input to a reconstruction stage in which the pattern models contained in the features are combined to produce a prediction of the original input. A feature can be used to predict a set of state probabilities for each of its inputs by making the best guess possible: that the probability set for an input is identical to its associated set in the pattern model. The extent to which a feature's model contributes to the reconstruction of a particular input is a function of two factors. The first is the probability produced by the feature during the detection stage, which is now part of the coding, and the second is the responsibility of the feature, r_{kn}, for that input. As each of these increases, so does the influence of the feature's predictions on the value of the input in the reconstruction.

Once the reconstruction stage is complete, the error between the predictions of the features and the original image is calculated. The precise value of this error is not important, however; what is important is knowing how the CFA model can be changed to lower the error. A standard way of doing this is to calculate the partial derivatives of the error function with respect to the each of the model parameters. Learning consists of evaluating the value of these derivatives during training and adjusting the model parameters by an amount proportional to their effect on the error. This is not precise since we only have the individual partial derivatives, but it has been shown to work well in many other learning algorithms.

A good way to evaluate how a learning method will behave is to look at its partial derivatives with respect to critical parameters and see what sorts of conditions will cause these parameters to increase or decrease. The most important feature parameters for competitive learning are the responsibilities, r_{kn}, we introduced in a previous section, which control the extent to which a feature considers a particular input to be part of its pattern. Below we show the simplified partial derivative of the model error with respect to the responsibility of feature k for input n, r_{kn}, where

- E_I is the total error over the entire input set I
- E_n is the error on input n considering the ensemble of features
- E_{kn} is the error on input n considering feature k alone
- N_D is the number of inputs in the data set
- C_1, C_2, and C_3 are additional factors which are outside the scope of this discussion

$$\frac{\partial E_I}{\partial r_{kn}} = C_1 r_{kn}(E_{kn} - E_n) + a_{kn}\left(\sum_{m=0}^{N_D - 1} C_2 r_{km}(E_{km} - E_m)\right) + C_3 \qquad \text{(EQ 7)}$$

If this derivative is negative, it indicates that raising r_{kn} will lower the total error; if it is positive, lowering r_{kn} will lower the total error. The most important and influential term in (EQ 7) is $(E_{kn} - E_n)$, which occurs twice weighted by the current responsibility. If feature k more accurately predicts input n than does the ensemble of features, the value of the term will be negative. If the opposite is true, it will be positive. The first instance of this term has a straightforward effect: if feature k is more accurate than the ensemble with respect to input n then r_{kn} is encouraged to increase. The second instance of this term is more subtle. The summation in brackets is a weighted sum over all inputs of the error difference term. If this sum is negative it indicates in essence that feature k should consider itself to be present in the input, as this would lower the total error. If a_{kn} is positive, increasing r_{kn} will increase the feature's output and thus will cause the feature to consider itself more likely to be present.

What all of the above shows is that in CFA the adjustment of critical feature parameters during learning is inextricably linked with the performance of that feature relative to any other features that are trying to use the same inputs. When the ensemble is presented with a training example, the feature that most accurately predicts a given input will end up with increased responsibility for that input. A feature which predicts an input with much less accuracy than others will receive reduced responsibility for that input. Over time, features will become localized to the patterns they predict best.

A side effect of the competitive formulation is that it provides an elegant way to include non-target training examples in the training set. If one is using an unsupervised learning method the training set typically can include only examples of the target class. Unsupervised learning methods focus almost exclusively on representation of the training set, and so would attempt to represent target and non-target examples alike if both were present. Since the method only sees target examples it has no opportunity to model the appearance of difficult non-target objects. CFA allows non-target examples by introducing the presence of a “virtual” ensemble of features that have both very low error and high responsibility for all inputs when a non-target example is presented. These features do not actually exist, in that they are never explicitly instantiated, but their virtual presence effectively lowers E_n for each input n. Learning proceeds as if features existed that performed well on non-target images, so from the perspective of all of the actual features there are now others which outperform them on these images. Competitive learning forces the actual features to refine their expectations such that they are less likely to detect non-target objects in the future. Using virtual features and non-target examples helps to ensure that features are detecting patterns that are characteristic of the target class in particular. The combination of unsupervised learning techniques together with the use of non-target training examples places CFA between the supervised and unsupervised learning camps. It is probably most accurate to call CFA a semi-supervised method.

One of the critical attributes of CFA learning is that it couples detection and representation. In CFA, representation is accomplished by the ensemble of features predicting the state of an input. If a feature does not consider itself to be present in an example, it does not attempt to predict the state of any inputs. If a feature does not accurately predict a pattern, other features will assume responsibility for detecting that pattern via competitive learning. Thus features must both detect and represent patterns accurately.

Building Hierarchies

We have discussed how competitive learning encourages features to decompose the input into independent, characteristic patterns. The other goal is to use the same mechanism to build hierarchies of higher-level features that represent the likely arrangements of those patterns. In order to build feature hierarchies we must be able to use the output of one feature as the input of another. Feature outputs are binomial in that a feature is either present or not present; o_k is the probability that the feature is present, so $(1 - o_k)$ is the probability that it is not. A feature output thus has the proper probabilistic meaning to be used as another feature's input. The output value is also a non-linear function of the inputs $\{i_{ns}\}$, which is critical as otherwise the rule of linear superposition would apply. Superposition states that any multi-layer hierarchy of linear operations is equivalent to some single linear operation, making hierarchy pointless.

Summary

The CFA learning method is designed to both automatically decompose the input space into separate characteristic patterns and automatically build hierarchies to unify these patterns. Decomposition is achieved via competitive learning between separate pattern detectors called features. Hierarchies are built by using multiple layers of features, with each layer trained on the output of the previous. CFA encourages features to detect patterns which are highly characteristic of the target class through the combination of a semi-supervised learning approach with a strong coupling between detection and representation.

2.4 Programmable Hardware

A Programmable Logic Device (PLD) is a chip which in some fashion allows a user to control the logic functions it implements. There are many types of PLDs, and these have found use in a wide range of applications[23]. When compared to custom hardware, the advantages of PLDs are shorter design cycles and the ability to re-program existing systems if a change in functionality is required. The chief disadvantages are a significant speed penalty (approximately 66-75% speed reduction) and greater cost in volume. When compared to a software implementation the advantage of programmable hardware is the potential for a significant speed increase, and the major disadvantage is a longer design cycle. For designs that are too large to fit on a single PLD, programmable systems comprised of a set of interconnected PLDs are used. In this section we present an overview of one type of PLD, the Field Programmable Gate Array (FPGA), followed by a basic discussion of programmable systems. We end with a description of the programmable system used in this work: the Transmogrifier-2a (TM-2a).

2.4.1 Field Programmable Gate Arrays (FPGAs)

Field-Programmable Gate Arrays are one of the most popular types of PLDs today. An FPGA

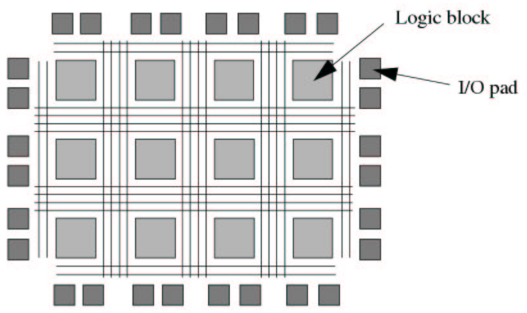

Figure 5: Structure of an Island-Style FPGA [24]

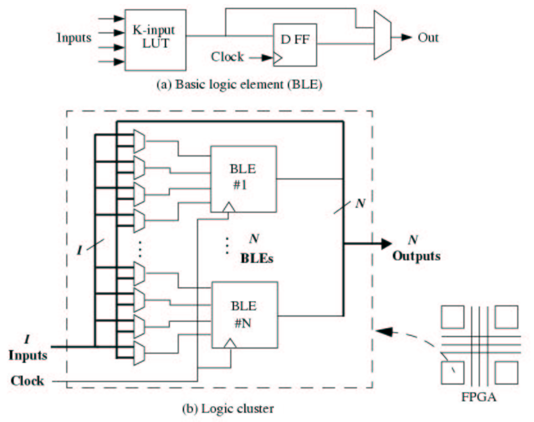

Figure 6: Detail of Logic Cluster Contents [24]

consists of programmable logic clusters connected by programmable routing. Figure 5 illustrates a typical island-style FPGA in which the "islands" of logic are separated with vertical and horizontal routing "channels". Figure 6 shows the contents of a logic cluster in more detail. Each block contains one or more Basic Logic Elements (BLEs) connected by local routing. A BLE often consists of a Look-Up Table (LUT) programmed with the desired function and a "D" flip-flop to implement sequential logic if necessary. FPGAs are the largest and most flexible PLDs because of this very general architecture.

2.4.2 Reconfigurable Systems

Reconfigurable systems are used to implement designs that will not fit inside a single programmable device. In many ways they are simply larger-scale versions of FPGAs; the typical system consists of a set of PLDs connected by programmable routing chips, just as an FPGA consists of a set of logic clusters connected by programmable routing.

2.4.3 The TM-2a Reconfigurable System

The Transmogrifier-2a [18][19] is an extensible programmable hardware architecture containing from one to sixteen boards in power-of-two increments. Each board contains two Altera 10K100 FPGAs [29], four I-Cube IQ320 Field Programmable Interconnect Devices (FPIDs) for inter-chip and inter-board routing, 8 MB of SRAM in four independent banks, and other housekeeping and programmable clocking circuitry. Its major uses are as a fast prototyping tool for large hardware designs and as a platform for reconfigurable computing research [20][21][22]. In addition, the circuits produced are large enough to provide critical benchmarks for ongoing research into next-generation FPGA architectures.

In this project we use a 16-board system. Video input and output cards are attached to I/O connectors on two of the boards. This allows the image data to be read directly from the camera and face detection results to be displayed on an attached monitor with no need for an intervening computer. The system clock frequency is set at 12.5 MHz; this is the highest frequency at which the SRAM operates reliably.

The Altera 10K100

As mentioned above, the TM-2a uses Altera 10K100 FPGAs [29]. These FPGAs are similar in structure to the generic FPGA presented in Section 2.4.1. Each contains 4992 Logic Cells (LCs), which are essentially equivalent to one of the BLEs described earlier. In addition, a 10K100 contains 24,576 bits of on-chip memory in 12 independent 2048-bit banks. Each bank may be separately configured to be 1, 2, 4, or 8 bits wide.

2.5 Object Detection Using Reconfigurable Systems

It is instructive to look at tasks similar to face detection that have been implemented using reconfigurable hardware. To our knowledge there is no hardware system, reconfigurable or otherwise, which performs face detection, but there are systems designed to perform other object detection tasks. In this section we review two approaches to Automated Target Recognition (ATR) on Synthetic Aperture Radar (SAR) data which have been implemented on reconfigurable systems.

2.5.1 ATR Problem Description

Although ATR uses the term “recognition”, by our earlier definition we would consider this to be a detection task and it bears many resemblances to standard visual detection problems. The SAR input data is very similar to a greyscale image where intensity indicates radar reflectance rather than visible light reflectance. Each target is represented by two binary templates: a “bright” template with 1’s where high reflectance is expected; and a “surround” template with 1’s where very low reflectance is expected. These templates must be correlated with a binarized version of the input data at each possible location, and peaks in the resulting correlation surface indicate the presence of the target. The input is binarized through a dynamic thresholding method which varies the threshold depending on the relative amount of intensity in the region under consideration. The intensity is measured by calculating the Shapesum, which is the result of correlating the “bright” template with the unthresholded input data. The basic steps to perform SAR ATR, then, are: Shapesum calculation, dynamic input thresholding, template correlation, and peak detection.

2.5.2 ATR Approaches

The first method was developed by Villasenor *et. al.* [26], using a dynamically reconfigurable platform. Dynamic reconfigurability indicates that the programmable hardware in the system can be partially or fully reconfigured during system operation in order to provide a greater range of functionality. This system uses 16x16 target templates, and since the hardware can be reconfigured to detect different templates the authors chose to avoid implementing general-case correlation hardware in favour of building circuits specific to each template. Customizing the hardware to the template significantly reduces the size of the circuit as unnecessary logic from the general case may be eliminated. This is particularly true for the SAR target templates, which are typically very sparse (10-15% populated). To produce additional efficiency, the authors combine multiple similar templates on a single chip and share Shapesum and correlation between them. This system implements dynamic thresholding by performing eight full correlations, each with a different threshold, in parallel with the Shapesum calculation. The Shapesum value is then used to select the appropriate correlation output.

The second system was developed by Rencher and Hutchings [27] on a reconfigurable system called SPLASH 2. They use a more complex ATR method dubbed “chunky” ATR, in which each target template is broken into 40 “chunks” representing important target features. These chunks are correlated separately and if more than half are present the target is also determined to be present. This allows detection even if the target is partially obscured. Rencher does not compile the template parameters into the circuit as he cannot dynamically reconfigure the device for each template. Instead, templates are stored in memory and loaded into a general 1-bit correlation circuit when needed. Rencher, however, introduces a major difference from Villasenor’s version by pipelining the Shapesum and correlation processes. The Shapesum is calculated first and passed to the correlation unit where it sets the SAR input data threshold. The disadvantages of performing the operations in serial are greater latency and somewhat larger comparators in the thresholding unit. The number of correlation units, however, is reduced from eight to one, and the threshold value is now more precise since the choice is not made from a set of fixed options. The drastic reduction in the number of correlation units is necessary as the general-purpose correlator will be much larger than Villasenor's sparse template-specific versions.

Rencher's implementation is the faster of the two, requiring only 18.5 ms to process one 16x16 template pair versus 52.5 ms for Villasenor (normalized to a 12.5 MHz clock). If we compare area, however, we see that Rencher requires approximately 18 times more area. If we consider the area-delay product (a standard measure for comparing hardware implementations) Villasenor's implementation comes out ahead by a factor of 7.5. This is most likely due to the efficiency of the template-specific and partially shared Shapesum and correlation hardware.

One point noted by both authors is the need to use mathematical operations that are as simple as possible. Complex operations such as multiplication do not use FPGA resources efficiently. The binary correlation units for SAR ATR use only addition and fixed shift operations, and thus are well suited to an FPGA implementation.

2.5.3 Discussion

Both of the above applications show that reconfigurable systems are excellent platforms for detection applications if the calculations required are numerous but simple. Programmable hardware is used most efficiently by simple operations and the less accuracy required, the more space there is to build in additional parallelism. The comparison between the two implementations reinforces the importance of creating hardware as specific to the task at hand as possible, and of using tools such as pipelining to the greatest advantage.

Chapter 3

Object Detection Framework

In this chapter we present the general object detection framework on which we base our face detection algorithm. The framework is a series of stages that may be adapted to suit the needs of many detection applications in addition to face detection. These stages are illustrated in Figure 7 with a face image. The first stage processes the input image with a set of G2/H2 filters, discussed

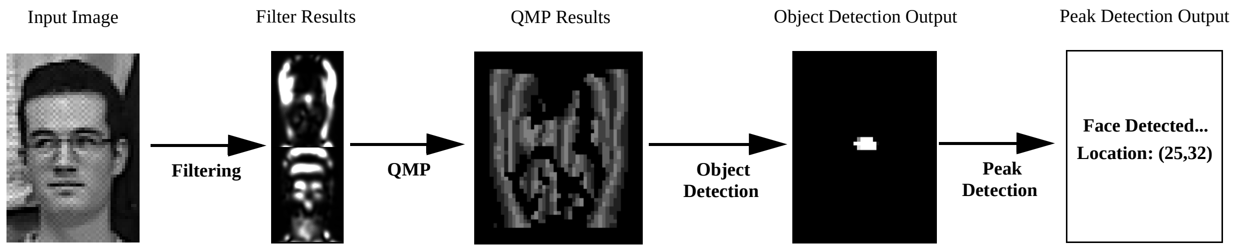

Figure 7: Object Detection Processing Sequence

in Section 2.2 above. The second stage converts the filter results to Quantized Magnitude/Phase (QMP) format, which we will describe in Section 3.2.2. The QMP values are used as the inputs to the final stage, which uses an ensemble of CFA features (described in Section 2.3.3) to calculate, for each position in the image, the probability that the target object is present. Finally, a thresholding and peak detection stage determines the precise object locations in the probability surface.

We first review the goals and assumptions of this part of the research and examine the advantages and disadvantages of choosing CFA as our learning algorithm. We then present each of the framework stages in detail. Finally, we discuss the success of the framework at meeting the stated goals.

3.1 Goals and Assumptions

In developing a general object detection framework, our goal was to provide a software suite that we could use to develop the face detection application and which could also be used to develop detection applications for a variety of target objects. We chose this general approach for two reasons: because it extends the applicability of the work beyond the single case of face detection; and because it helps to ensure that face-specific human biases have minimal influence on the choice of detection strategy. To support a range of objects the processing stages are highly parameterized, since each particular application will require different types of information at different levels of accuracy.

We assume that significant variation in object scale and in-plane rotation will be handled outside of the framework by scaling or rotating the input image. The amount of variation that can be handled within the framework will depend on the object's appearance and on the training set used.

3.2 Image Processing

The first two stages in the framework process the incoming image and convert it to a format suitable for use with CFA. The image is convolved with a bank of oriented and scaled G2/H2 filters, and then the filter results are converted to Quantized Magnitude/Phase (QMP) representation. In this section we present the details of these steps and how they affect the framework as a whole.

3.2.1 G2/H2 Filtering

The first processing step is to apply a set of oriented and scaled G2/H2 filters. The precise orientations and scales used will depend on the application in question, but in general these will be chosen such that they capture important structure in the target object. We chose this filtering method because of the need to resolve a set of interrelated problems caused by the assumption of uncontrolled lighting, by the choice of learning algorithm, and by the goal of an efficient hardware implementation. Assuming uncontrolled lighting implies that the intensity value of any individual pixel has little meaning, as changes in lighting brightness and direction could cause it to vary considerably. CFA requires that the algorithm inputs are in the form of probabilities, which, in contrast, must have very well-defined meanings. This makes raw pixel intensity values unsuitable as direct inputs to CFA. We must ensure in addition that any image processing we do may be implemented efficiently in hardware, or otherwise we will violate one of the primary goals of this research. While G2/H2 filtering does not solve all of these problems, it does begin to address them.

The filters have no DC response, making them insensitive to additive scalar lighting changes, or lighting brightness. At each location they analyze the intensity variation over a local set of pixels to derive texture information that is much more meaningful than a single intensity alone. The G2/H2 filters, as we discuss in Chapter 2, are also very efficient due to the combined properties of X-Y separability and orientation-steerability.

3.2.2 QMP Conversion

While the individual filter results now have more meaning than individual pixels, they are not the probabilities required as inputs to CFA. To produce these probabilities we convert each G2/H2 response to a format that we designed to preserve the important information in each filter result and to be both calculated and stored efficiently. This format is called Quantized Magnitude/Phase (QMP) format. It is important to note that this choice of representation is a crucial factor in the efficiency of the final hardware implementation.

In order to discuss how QMP works, we must introduce the concept of filter response phase and magnitude. G2 and H2 are a quadrature pair, which means that in the frequency domain the phase response of H2 is shifted 90 degrees with respect to G2. This relationship produces an interesting property: we can use a linear combination of G2 and H2 to create a filter with the same magnitude response but arbitrary frequency phase shift. If we apply both filters at a given location in an image, we can use the two responses to determine the filter phase which would receive the strongest response magnitude. This is often simply called the phase of the response. Response phase is a useful description of local image texture that is invariant with respect to multiplicative changes in lighting, or lighting contrast. Magnitude is not completely irrelevant, however, since in smooth areas of the image the filter response will be too weak for phase to be meaningful, and we need to detect this condition. The phase and magnitude of the G2/H2 response are calculated simply as:

$$\|\mathrm{G2/H2}\| = \sqrt{G^2 + H^2} \qquad \text{(EQ 8)}$$

$$\Phi(\mathrm{G2/H2}) = \mathrm{atan}\left(\frac{H}{G}\right) \qquad \text{(EQ 9)}$$

This is illustrated graphically in Figure 8.

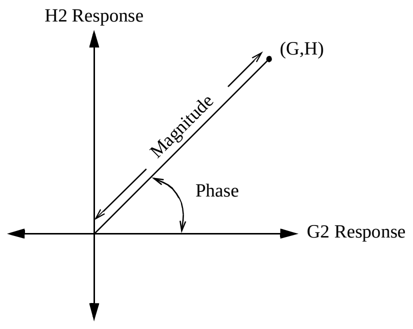

Figure 8: G2/H2 Phase and Magnitude Calculation

The key to QMP is combining phase and magnitude information in a way that is compact, computationally cheap to calculate, and, when combined with the CFA object classifier, makes detection extremely efficient. While we know the phase angle provides useful information, it is unclear how the actual value should be calculated and used. From a hardware perspective an accurate phase value is expensive to represent and even more expensive to calculate, as it would involve evaluating the computationally complex function $\operatorname{atan}(H/G)$. Instead we divide the phase space into a set of bins. A response phase angle can now be encoded using only the bin number into which it falls. If there are n phase bins and n is divisible by four (to ensure the same number of bins in each quadrant), the calculation of the correct bin in hardware may be accomplished with two absolute value operations, $\left(\frac{n}{4}\right) - 2$ constant multiplications, $\left(\frac{n}{4}\right) - 1$ compare operations, and minimal additional logic to evaluate the signs of the G2/H2 responses and adjust the bin number appropriately. The number of bins required depends on the accuracy needed by the application.

To incorporate magnitude information we add an extra “bin” to represent the case when the response is below a fixed threshold. Although this means that the framework will not detect a target object with extremely low contrast, these cases should be both rare and unimportant. Calculating the vector’s magnitude requires squaring both the G2 and H2 responses. If either G2 or H2 alone is greater than or equal to the threshold, however, there is no need to perform the calculation. We will only need to provide a multiplier large enough to square the bits representing values below the threshold.

Using the QMP representation is critical to hardware efficiency. Once calculated, the QMP value is very compact. If there are there are n phase bins plus one low-magnitude bin, we only need ceil(log2(n+1)) bits to store each result. In an application that used eight bins of phase accuracy, we would only need four bits per QMP value. This is a savings of 12 bits from the storage required for the G2/H2 pair used to derive the QMP value. QMP is also an efficient input to CFA. As we will discuss in Chapter 5, quantizing the filter output into one of a set of bins removes the need for any multiplications in the face classifier network.

One final advantage of working with phase information is that we can perform an interesting trick that again improves tolerance of lighting changes and introduces some invariance with respect to background shading. If we reflect phase angles into the upper-left-hand quadrant we retain G2/H2 response ratio information while discarding response polarity. Figure 9 illustrates the reflection operation. **A** and **B** are the original G2/H2 response vectors, and **A’** and **B’** are the vectors after reflection. The most important implication of phase reflection is that we can reliably detect the border between objects and background so long as there is some brightness difference between them. This is true even if the polarity of the border changes along its length or between object instances. The disadvantage to this is that by increasing the tolerance of the detection system to polarity variation we may increase the occurrence of false positives in the final application. Phase reflection does not save any significant amount of hardware over a non-reflected implementation with the same amount of G2 vs. H2 response discrimination; only the G2/H2 response sign check can be discarded.

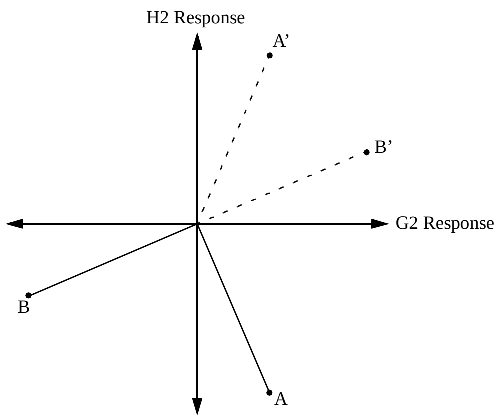

Figure 9: Phase Reflection

3.3 CFA Classifier

Once the first two stages process the input image, they pass the results to the CFA-based object detector. This detector consists of one or more CFA features which together generate a probability at each location in the image indicating the likelihood that a face is present. In Chapter 2 we discussed the important properties and advantages of CFA as a learning algorithm for detection problems. In this section we describe how we implemented the CFA learning environment, and we discuss in what ways the implementation succeeded and failed.

3.3.1 Training Strategies

The heart of CFA is its competitive learning formulation designed to decompose an object’s appearance into a set of characteristic sub-patterns. Each sub-pattern is represented by a CFA feature. This feature maintains a probabilistic representation of the pattern’s structure which it uses to detect the pattern in an input image. The goal of the training process is to both optimize each individual feature’s pattern representation to improve its detection accuracy, and to enable competition between features to determine the optimal number and scope of sub-patterns. In this section we discuss three aspects of our CFA training implementation that enhance its flexibility, accuracy, power, and feasibility.

Improving Flexibility and Accuracy

In the most straightforward implementation of CFA, all of the training set images would be the same size and would be cropped such that the target object is always in same position. This is a common approach for many learning algorithms, both unsupervised and supervised, because it greatly simplifies the training process. We have developed an alternate implementation that structures the CFA learning environment to allow any image size or object position, and in the process promotes greater detection accuracy.

When an input image is presented to the algorithm we create multiple copies of the existing features such that there is one copy of each feature located at each position in the image. We call this process *feature replication*. Patterns will be detected regardless of their position, since every feature has a copy at every image location. Even though the all of the copies of a given feature are identical, however, they are considered separate for the purposes of competitive learning. All feature copies, regardless of which original feature they were copied from, will compete with each other to detect and represent the input just as separate features would. As parameter updates are calculated, all changes that apply to a feature's copies are summed and applied to the original feature. Readers familiar with neural networks will recognize this as similar to weight sharing, with the notable exception that the effective number of neurons changes with the image dimensions.

Feature replication has three major implications. It allows us to use images of any size as input since the number of feature copies can change with the image dimensions. It also allows us to use images containing any number of target objects appearing at any position and allows patterns represented by different features to move with respect to one another with no constraints. Lastly, it promotes detection accuracy. Consider that copies of the same feature located near each other will be using many of the same inputs. If a characteristic pattern is present, many of the copies around its location will likely respond, creating a peak in the feature result surface. Competitive learning will encourage the more successful copies to have a greater response while suppressing the others. As learning proceeds, the response peak will narrow and heighten; narrower, higher peaks result in more accurate detection.

```
DO
{
    “freeze” all existing feature parameters
    create new feature
    train the new feature on weighted data until it learns a pattern reasonably well
    add new feature to existing features and “unfreeze”

    IF(more than one feature)
    {
        “unfreeze” all features

        DO
        {
            train once through entire training set
            check if we should remove any features
        }UNTIL(we reach a fixed number of iterations or we remove a feature)
    }
}UNTIL(we have removed a feature N iterations in a row)
```

Figure 10: Pseudocode for Iterative Feature Addition/Removal

Enabling Multi-Feature Training

While the CFA formulation allows any number of separate competing features, it does not specify how to determine how many features are required. One good option would be to perform multiple training runs, each with a different number of features, and statistically analyze the results to determine the optimum number. In practice, however, we found that if we simply began training with multiple concurrent features, the feature that first started to detect a pattern immediately prevented the others from learning anything. To work around this problem we implemented an iterative method for adding and removing features.

Figure 10 describes this process in pseudocode. In each iteration we first “freeze” any existing features, meaning that we fix their parameters and do not allow them to learn. We then create a new randomly initialized feature. We train this feature by itself on data weighted to emphasize areas on which the current ensemble has the greatest error. We train this feature until it has learned a pattern reasonably well, which we evaluate by recording the feature’s maximum output. Assuming the new feature is not the very first to be added, we then un-freeze the whole ensemble and train them together competitively. As we proceed through the training set we keep track of the maximum response each feature produces. If the maximum response for a feature over the set is below a given threshold, we assume that it has been forced from its pattern by another feature and should be removed. We continue to train until either we have removed a feature or have made a fixed number of passes through the training set. We then attempt to add another feature. The process is repeated until we remove a feature in each of a number of successive iterations. The precise number of iterations is another parameter to the process.

This iterative method has two major drawbacks. First, it is prone to becoming trapped in local minima that are found while training with a small number of features, and that cannot be escaped by adding more. Second, it introduces several additional training parameters which have no *a priori* reasonable values and yet can have significant effects on the final result. Nonetheless, it provides a reasonable solution to the problem of determining the number of features, given that we cannot simply train multiple features from scratch. As we discuss in the testing section below, we were able to find settings with which this method correctly determined the number of features for an artificial test data with two independent patterns.

Modifying Feature Scope

The CFA formulation assumes that every feature has some prediction for every input. This is not feasible in an implementation, however, as we must limit the scope of a feature in order to store its parameters in a reasonable amount of space and evaluate its results in a reasonable amount of time. In this implementation, each feature has a current scope defined by a rectangular area. For good efficiency we would like to limit the scope of a feature to the minimum rectangle required to encompass its characteristic pattern. On the other hand, to perform flexible learning we would like to make sure that no characteristic pattern is truncated by a feature's scope. We need to be able to both shrink the scope of features that are much larger than their pattern and increase the scope of features if the patterns are currently being truncated

To do this we periodically examine each feature during training. If all the feature's effective "weights" along one edge of the scope rectangle are vanishingly small, then the connections along that edge are removed and the feature shrinks. If there is a weight along an edge that is larger than a given threshold we assume that the pattern could be extended in that direction and we add a set of connections to that edge of the scope. In this way the scope of a feature will adjust to the scope of its pattern during learning. This method performed well during testing, as described in Section 3.3.3 below.

3.3.2 Hierarchy

If an object is decomposed into multiple features, then hierarchy needs to be built to unify the

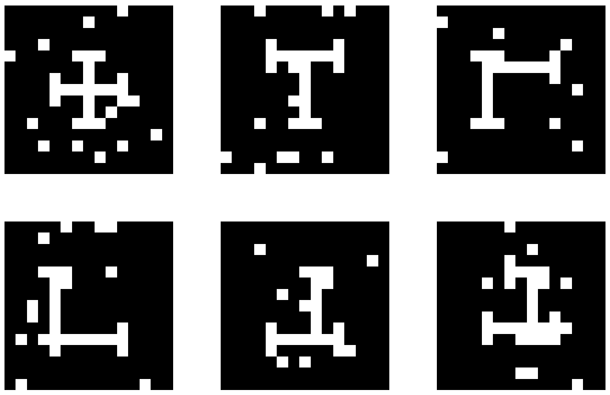
Figure 11: Sample Input Arrays

a) Final Probabilties **b) Final Responsibilities**

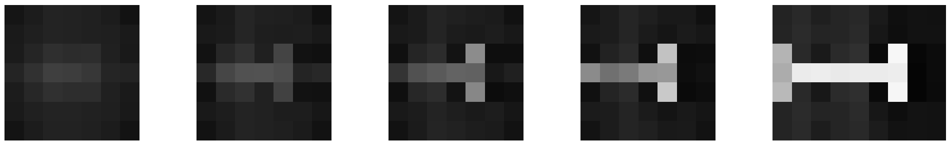
c) Progression of Horizontal Feature Probabilities During Learning

Figure 12: Features Learned and Learning Progression During First-Level Training

features into a single object detector. This framework supports an iterative method of hierarchy building. The process starts by learning an initial layer of features trained using the feature adding/removal algorithm described above. Once learning has converged, the layer is “frozen” and the procedure is repeated using the outputs of the newly trained layer as the inputs to the next. The hierarchy is complete when learning for the current layer completes with only a single feature.

3.3.3 Testing

Once the CFA learning environment was fully implemented we tested its performance using an artificial data-set. The artificial data consisted of a 15x15 binary image containing a variable cross-hair pattern and 10% noise. Figure 11 shows several sample input arrays. The cross-hair consists one vertical bar that randomly shifts back and forth horizontally and one horizontal bar that randomly shifts up and down vertically. Each bar has a main shaft five pixels long with perpendicular three-pixel caps at either end.

Training at the first level using the iterative feature addition/removal algorithm produced two features, the structures of which are shown graphically in Figure 12. Each feature started with a 7x7 scope and with randomly initialized parameters. We can see that the features have correctly decomposed the input into its independently varying patterns, and that the feature scopes have adjusted to fit these patterns. The responsibility maps show an accurate and distinct separation of the information represented best by one feature from that represented by the other. Figure 12 also shows the progression during learning of the horizontal bar model. We can see how the CFA feature refines and extends its model to more accurately account for the pattern it detects.

One discouraging result to come out of the first-level testing was the sensitivity of the CFA decomposition to learning parameter values, particularly regularization strengths and iterative addition/removal parameters. Although the algorithm was able to successfully decompose the artificial input, it only did so after considerable tweaking. To make matters worse the number of different parameters and the lack of a simple measure of learning performance make it difficult to create a method to automatically find good parameter values. We discuss the implications of this at the end of the chapter.

Training the second level of hierarchy produced similar results but with even greater evidence of instability. The results of a successful training run are shown in Figure 13. The two images represent the predictions of a single feature for the position of the vertical and horizontal bars. We can see that it has correctly captured the movement of each bar. These results came, however, only after several hundred randomly initialized training runs and after unreasonable regularization parameter values were used to essentially force the feature to detect both bars or not learn at all. In all other cases the feature would detect the position of one bar precisely and ignore the other.

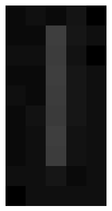
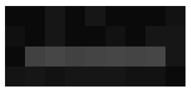

a) Horizontal Bar **b) Vertical Bar**

Figure 13: Second Level Feature Predictions for First-Level Feature Positions

3.4 Peak Detection

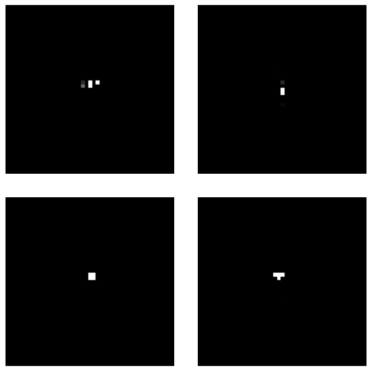

Figure 14: Face Probability Surfaces

The output of the CFA feature ensemble is an object probability surface. We need to take this array and determine where the objects, if any, are located. The first step is to discard all values below a set threshold. This threshold determines the minimum output value required to indicate the presence of a face. Next we locate peaks in the surface. Although the CFA learning environment is constructed to encourage highly localized responses, there will still often be a small area around the most accurate object location where output probabilities remain above the threshold. Figure 14 shows four example probability surfaces from the final stages of face training, discussed in Chapter 4. To distinguish the points of best response, we employ a simple but robust peak detection method. This method iteratively finds the highest response over the entire surface, which is guaranteed to be a peak, and then discards that response along with all those in a surrounding rectangle. The size of this rectangle is determined by the bounding box of the detector region of interest; in the case of a single feature, this would be the feature's scope. The algorithm ends when all values on the surface have been discarded. This method works well in nearly all circumstances.

3.5 Summary and Discussion

The goal of this stage of the research was to design and implement an object detection framework based on CFA that could perform accurate object detection in a manner suitable for hardware implementation. We included this stage for two reasons. First, we recognize the many advantages of approaching face detection from an unbiased object detection standpoint. Second, it extends the usefulness of our work beyond face detection alone. We separated the object detection task into four stages: G2/H2 filtering, conversion to QMP representation, calculation of object probabilities, and peak detection.

G2/H2 filtering extracts meaningful local texture information, enhances the system's tolerance to lighting changes, and is efficient to implement. As we show in Chapter 5, the separable filters require approximately half of the hardware area of a non-separable implementation with the same throughput.

The QMP representation, though seemingly simple, turns out to be one of the most important components of the system. A QMP value combines the magnitude and phase information from one G2/H2 result pair in a way that conserves important information while providing excellent lighting tolerance. The quantization calculation is efficient and the representation is very compact. Perhaps most important, however, is that quantization greatly improves the hardware efficiency of CFA by eliminating multiplications.

The framework calculates object probabilities using an ensemble of CFA features. We chose CFA because it has several potential advantages over other methods. This implementation of CFA realizes its key potential benefits: competitive, semi-supervised learning; input decomposition via multiple features; and hierarchy building. Testing showed that the system could successfully decompose an artificial data-set into its two separate components.

Testing also discovered several difficulties with the CFA approach. The first of these is a serious flaw in the CFA formulation: it is unable to successfully train multiple features in concert. We worked around this difficulty by developing an iterative feature addition/removal algorithm which initializes new features before allowing them to compete with existing ones. This approach, however, is likely to become stuck in local minima and the results it produces are very unstable with respect to training parameters. The instability problem currently has no solution, and it slows the training process by requiring large numbers of iterations over the parameter values. It is unlikely that the current CFA formulation would be able to perform a useful decomposition of more complex data. This limits the feasible complexity of the face model to a single feature.

A somewhat more subtle problem is the lack of a useful measure of learning performance. When using supervised learning, one can measure the error between the model outputs and the provided target outputs. When using unsupervised learning, one can measure the error between the training example and the model's reconstruction of that example. When using CFA, however, there is no "ground truth" to compare with. There are no target outputs. Reconstruction error seems to be a good choice until we consider that CFA only tries to represent patterns in the data that may be reliably detected. By ignoring unreliable portions of the data, a CFA feature could increase detection accuracy while also increasing reconstruction error. The most relevant measure is the detection accuracy, but this is difficult to quantify due to the trade-off between false negatives and false positives. The practical result of this problem is that it is difficult to create a simple method to automatically find reasonable parameter values that does not itself include a number of arbitrary parameters.

Despite these setbacks, and in some ways because of them, our implementation and testing provided valuable information for future work to improve CFA.

Chapter 4

Hardware-Ready Face Detection

In this chapter we present the face detection algorithm developed and trained using the CFA-based framework described in Chapter 3. The overriding goal of this design is to extract the most useful information from the input image with an absolute minimum of operations. The fewer operations we require, the smaller and faster the hardware design will be; if we do not pay close attention to algorithm complexity, we face the possibility of the design simply not fitting on the hardware platform. We also must recognize the training problems of CFA that we discussed in Chapter 3. If we attempt to make the model too complex, we may either be unable to learn properly or require too much time to do so.

We first review the framework stages and the parameters that we must determine for each, and then look at the design of the first two stages, G2/H2 filtering and QMP conversion. We next consider in detail the face detector training process. Finally, we present accuracy results for the system and discuss its overall performance.

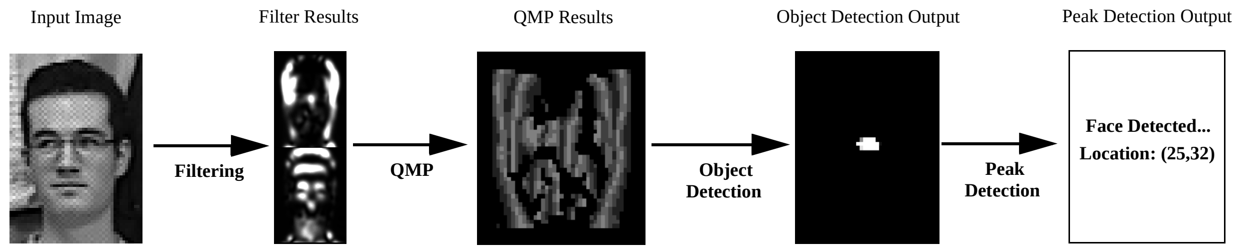

Figure 15: Object Detection Processing Sequence

4.1 Review of Framework

Figure 15 reviews the stages of the object detection framework. There are three stages that must be customized to the specific application: G2/H2 filtering, QMP conversion, and object detection. The parameters of the first two stages are relatively simple. For the filtering stage, the parameters to consider are the orientation and scales (sizes) of filters that will be used. For the QMP conversion stage, the key parameters are the number of phase bins, the low-magnitude threshold value, and whether or not to use phase mirroring to ignore filter polarity.

The design of the object detection stage is more complex. We focus below on the composition of the training set and details of the training algorithm which improve both the speed with which learning proceeds and the accuracy of the resulting detector.

4.2 Filtering and QMP Conversion Parameters

The goal when choosing filter parameters is to account for as much of the important frequency spectrum as possible with as few and as small filters as possible. It is difficult, however, to determine what face information, and thus what frequency range, is important before we train the detector; this is the job of our learning algorithm. Since 9x9 filters are the smallest feasible size for G2/H2 [16], and the 0 and 90 degree orientations are the simplest to implement and together cover approximately two-thirds of the orientation spectrum [16], we used these as our initial choice. We discuss in Section 4.3 how we then adjusted feature scope to find a reasonable spatial frequency range.

When choosing QMP parameters, we would again like to capture the information we need as simply as possible. For QMP quantization we use the polarity-invariant phase reflection described in Chapter 3 and four phase bins centered at 0, 30, 60, and 90 degrees. Phase reflection allows us to use information from the face/background border, and the four phase bins provide what would seem to be a reasonable amount of phase resolution. We chose a QMP magnitude threshold of 8, which is the value at which approximately 60% of the filter results from our training set fell into the “low magnitude” bin.

4.3 Object Detection Training and Testing

In this section we describe the design and training of the CFA face detector. We first describe our choice of the number and scope of CFA features used. We then look at the composition of the training data and several training strategies that we implemented to improve learning speed and detection results.

4.3.1 Number and Scope of Features

As we described in Section 3.3, CFA can decompose its input into a set of features using an iterative algorithm. Results from the same section, however, show that the final number of features used was very sensitive to learning parameters. We concluded that CFA would not be able to accurately perform this decomposition on complex data in a reasonable amount of time. Given these results, we chose to limit the CFA face detector to a single feature. Although doing so reduces the potential accuracy of the detection system, it will also reduce the difficulty of the learning problem and thus the time required to train the detector.

Face Size	False Positives Per Non-Face Image
48x45	12.6
39x37	11.5
32x30	11.9
25x23	13.9

Table 1: Accuracy vs. Face Size

Given that we are not going to attempt multi-feature decomposition on faces, we can fix the feature scope before training to be the size of the faces in our training set. As with other parameters, the choice of face size is driven by two needs: the need to capture important information, and the need to reduce the complexity of the system. As we change the size of the training set faces, we change the resolution at which we sample those faces and also shift their spatial frequency content. Lowering resolution reduces the complexity of the CFA feature but also potentially reduces accuracy. Shifting frequency content changes the responses we will get from our 9x9 G2/H2 filter pairs, and could reduce accuracy if these filters no longer capture important face information. The only way to find the correct balance between complexity and accuracy is to sample how detection accuracy changes as we vary face size. The metric we used was the number of false positives encountered for a detection rate of 90%. Table 1 shows the results for four face sizes. We began with the bounding box of an existing face, 48x45, and then reduced this size by approximately 20% at each step. The number of false positives remains quite flat until 25x23, at which point it increases significantly. We chose the next highest resolution, 30x32, for the implementation. This analysis, performed at the start of this research, did not have the benefit of the full current training set, of full training parameter optimization, or even of all of our training algorithm modifications. Any future implementations should revisit this decision in light of these changes.

4.3.2 Face and Non-Face Sets

In total, we used 770 face images containing approximately 119 different people[30][31]. We separated ten percent of these for use as a test set, and used the rest to train the face model. We created three versions of each face image, each randomly scaled within $\pm 10\,\%$ of the standard model size of 32 pixels high by 30 pixels wide. We made no effort to similarly introduce random variation in head tilt. We instead selected the training images to include subjects in natural rather than arranged poses, such that the variation in head position present in the set would be representative of that encountered during operation. The images include the left and right borders of the face so as to take advantage of QMP polarity-invariance. The training and test sets are intentionally difficult, including noisy images, uncontrolled lighting conditions, and moving subjects.

We also gathered 371 non-face images and similarly split them into training and test sets[32][33]. The images are densely textured examples of foliage, rocks, fabric patterns, and other complex materials. These are ideal for testing face detection performance as their complex fractal structure inevitably generates face-like false positives. We scaled each image to six different sizes to take advantage of the multi-scale nature of the patterns and increase the number of non-face examples.

4.3.3 Feature Initialization

When using any iterative learning strategy there is always the question of how to initialize the model parameters. Typically they are generated randomly from some reasonable distribution. In the case of CFA we have a particularly difficult problem. A feature will only learn a pattern if it already detects some portion of it, however minimally. This is not a problem in theory; given enough randomly initialized features we will eventually find one that coincidently resembles a pattern in the input. It is, however, a problem in practice since we cannot spend hundreds of training runs waiting to generate the correct pattern. Instead, we randomly choose one example from the training set and use it to bias the initialization towards that example’s pattern. To avoid moving the model to a strong local minimum, the bias is very slight. In practice, this approach eliminated the need for multiple random restarts.

4.3.4 Fixation and Repetition

In order to speed the learning process we introduced two strategies. The first of these constrains feature replication, described in Section 3.3, to the immediate area of the face. Normally replication would cover the entire input image, but by restricting it to the face we do two things: reduce the number of feature copies and thus reduce the number of results and training updates to be calculated; and simplify the training problem by simplifying the input data and restricting competition between feature copies. Both of these effectively shorten the training process. We call this strategy *face fixation*, as it prevents the training process from considering information beyond the face. As the feature begins to learn its characteristic pattern better, the fixation is relaxed to provide the full benefits of feature replication.

The second strategy increases the impact of certain training examples by presenting them multiple times in succession. The number of times the example is presented is inversely proportional to how well the feature currently performs on that example, as measured by the reported detection probability. We call this strategy *face repetition*. Repetition essentially causes the training process to “stare” at difficult examples, increasing the effective learning rate.

These strategies have a remarkable effect on learning speed. Fixation alone reduces the number of training iterations by approximately 50%. Repetition reduces training time by a further 75%. In both cases there was no significant reduction in accuracy.

4.3.5 Bootstrapping

Bootstrapping is a well-known training technique that uses the current performance of the system to dynamically change the composition of the training set. It effectively makes the training problem more difficult by removing examples on which the system already performs well, thereby increasing the proportion of difficult ones. This is particularly useful for detection problems, as bootstrapping automatically identifies good non-target examples in the training set.

Detection Rate	False Positives per Image Location without Bootstrapping	False Positives per Image Location with Bootstrapping
~90%	4.02×10^{-5}	3.87×10^{-6}
~80%	7.55×10^{-6}	7.87×10^{-7}

Table 2: Comparison of False Positive Rates for Bootstrapping vs. No Bootstrapping

While the repetition strategy discussed above focusses mainly on improving training speed, bootstrapping focusses on improving the quality of the results. As shown in Table 2, once bootstrapping was included in the learning process, the number of false positives for a given detection rate decreased by almost precisely an order of magnitude.

4.4 Detection Accuracy Results

Table 3 shows how face detection accuracy varies with respect to both false positives and false negatives as the face classification threshold is varied. Given the difficulty of the images used to train and test the system, these results are excellent.

Threshold	Detection Rate	False Positives per Image Location
0.11	90.9%	5.80×10^{-6}
0.21	90.3%	3.82×10^{-6}
0.52	87.0%	1.91×10^{-6}
0.95	80.9%	7.87×10^{-7}

Table 3: Detection Accuracy vs. Face Classification Threshold

Table 4 shows the accuracy results for other similar face detection methods on their own test sets (from [12]). Although these should not be directly compared with our results given that different test images were used, we can see that on average for a comparable detection rate we have approximately an order of magnitude more false positives. Since our face classifier is much simpler than any of those given in Table 4, this may indicate that our test set is not as difficult as those used by the other methods.

Method Authors	Detection Rate	False Positives per Image Location
Schneiderman et. al. [12]	91.2%	1.66×10^{-7}
Sung et. al. [13]	84.6%	1.81×10^{-7}
Rowley et al. [11]	86.6%	9.51×10^{-7}

Table 4: Examples of Accuracy Performance for Similar Methods (from [12])

4.5 Discussion

The most important result we derived from this portion of the research is that we can perform reasonably accurate face detection using only very simple operations. We are performing minimal pre-processing and using the equivalent of a single artificial neural network neuron for face classification. Other detection strategies based on neural networks using pixel values as input require two layers of neurons for a total of 20 neurons or more [10][11]. Since each neuron requires both storage for its weights and computation to evaluate its activation, reducing the number of neurons so dramatically greatly increases efficiency. That we can do so and maintain detection accuracy is evidence that both the pre-processing strategy and detection classifier were good choices.

Another important result is the demonstration that CFA can perform face detection at all. This is the first application of the CFA learning formulation to real-world data, and the model it learns, represented partially in Figure 16, is both intuitively pleasing and reasonably accurate. Although we have not demonstrated the multi-feature decomposition capabilities of CFA, it is important to remember that virtual features and feature replication make use of competitive learning even in the single-feature case, and both of these training strategies operated as expected.

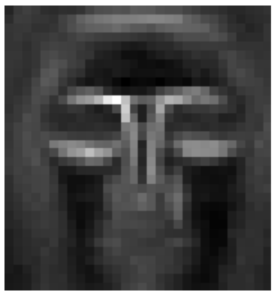

Figure 16: Probability of H2 Response (normalized to [0,255])

The major difficulty we experienced in the move from artificial data testing to more complex data was a substantial increase in learning time. Even given the initialization, fixation, and repetition strategies discusses above, a single training run required approximately five to ten days of computer time on a 300 MHz SPARC, depending on the specific training parameters used. This is largely due to the complexity of the CFA learning problem; while CFA’s competitive, semi-supervised learning provides some interesting advantages, it also needs many more iterations to train than more traditional learning methods. This is another problem CFA will have to overcome if it is to be useful in complex situations.

Chapter 5

Hardware Implementation

In this chapter we present the hardware face detection system. We begin by reviewing our goals for this implementation and giving an overview of the system as a whole. We then describe each individual processing unit in detail. At the end of the chapter we provide performance results and comparisons versus both a serial implementation of the algorithm and serial implementations of other face detection algorithms.

5.1 Goals

The goal of this implementation was to achieve full frame-rate face detection using the Transmogrifier 2a and the algorithm described in Chapter 3 and Chapter 4. We also wanted to be able to detect any number of faces and be able to detect them over the full range of scales from the smallest detectable face to the largest that fits in the image. Assuming a 320x240 input image and eight scale steps gives approximately 313644 pixels to process for each frame of video. One frame arrives every 33 ms. Given the 12.5 MHz TM-2a clock, the system will need an effective throughput of one pixel every 1.33 clock cycles to keep up with incoming video. To meet this constraint, the primary design requirement for the units described below was that each should be able to both consume and produce one piece of data every cycle, whether that data is a pixel, a filter output, a QMP value, or a face probability. This ensures that data will “stream” efficiently through the system and allows each unit to be unproductive for up to one out of every four cycles.

5.2 Overview

Figure 17 shows a block diagram of the system. Image data in the form of pixel greyscale values flows in from the video input unit, through a scaling unit, and to the X and Y stages of the separable filter pairs. Filter results are converted into QMP format and passed to the Face Detection Unit (FDU), which calculates the face detection probabilities. As face probabilities emerge from the FDU they pass through a peak detector which finds local maxima. The location of any maxima are passed to the display unit where the marked face locations are merged with the original input and shown on the monitor.

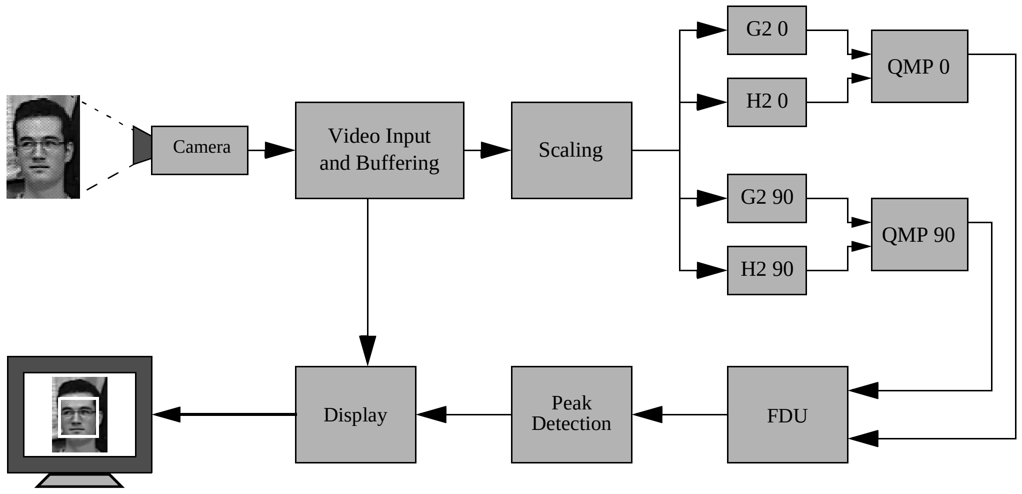

Figure 17: Block Diagram of Face Detection System

5.2.1 Flow Control

This system was designed to keep data flowing within and between the various units with minimal need for buffering and retrieval. Even so, each unit has periods during which it is unable to receive or unable to send data. To ensure that these delays are handled properly we implemented a synchronous Data Request/Data Ready handshaking protocol between all units. The Data Request signal indicates that the receiving unit is ready to accept new data, and the Data Ready signal indicates that the sending unit has valid data to transmit. If both of these signals are high during a particular cycle, then we consider the data to be successfully transferred.

5.2.2 Hardware Description Language

All of the hardware in the system is described using the Altera AHDL language.

5.3 Video Input

The video input unit receives data from an external frame grabber board containing a Brooktree 812 chip. The video source is an RCA video camera/recorder. In order to avoid interlace tear on moving objects, only the odd field is used and pixels are horizontally averaged to produce a 320x240 final image. Pixels are placed in two 1KB circular FIFO buffers, one for the display unit and one for the face detection pipeline. These buffers cannot hold the entire image, but are instead intended to allow for moderate delays in either the display unit or face detection path without loss

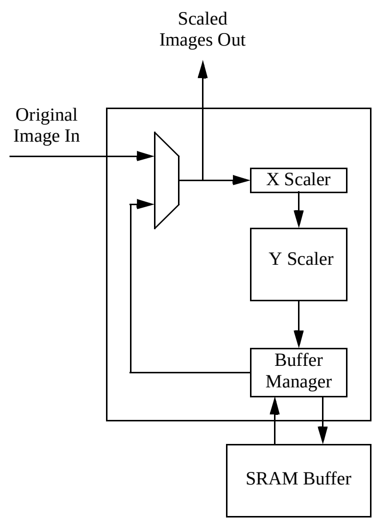

Figure 18: Structure of Scaling Unit

of pixels.

5.4 Scaling

As we discussed in Chapter 3, the object detection framework assumes that significant scale variation is handled by scaling the input image and reapplying the face detection algorithm. To achieve this in hardware, the scaling implementation produces 7 iteratively scaled images in addition to the original input image. Scaling proceeds at the desired one pixel per cycle throughput while introducing fewer than ten cycles of latency.

The most important parameter of the scaling unit is the scale 'step' or scaling factor: the amount by which the image dimensions change between successive scaled versions. We chose a scale step of $\sqrt[3]{2}$. This value has three important properties: it is small enough that the face detector, trained for +/-10% scale variation, can detect faces that appear between scale steps; it may be approximated as 1.25, which is a relatively simple scale factor to deal with in hardware; and every three steps we reach a factor of 2, which we can calculate efficiently and precisely and is a generally handy number for hardware purposes.

We perform scaling in by placing two units in series in front of the face detection pipeline. Each of these units takes a single image as input and produces three images as output. The first of these images is simply the original image. The second and third are iteratively scaled versions. The only difference between the two units is the scaling factor each uses. The first unit shrinks an image by a factor of two in each dimension. The second unit fills in the large scale jumps between factors of

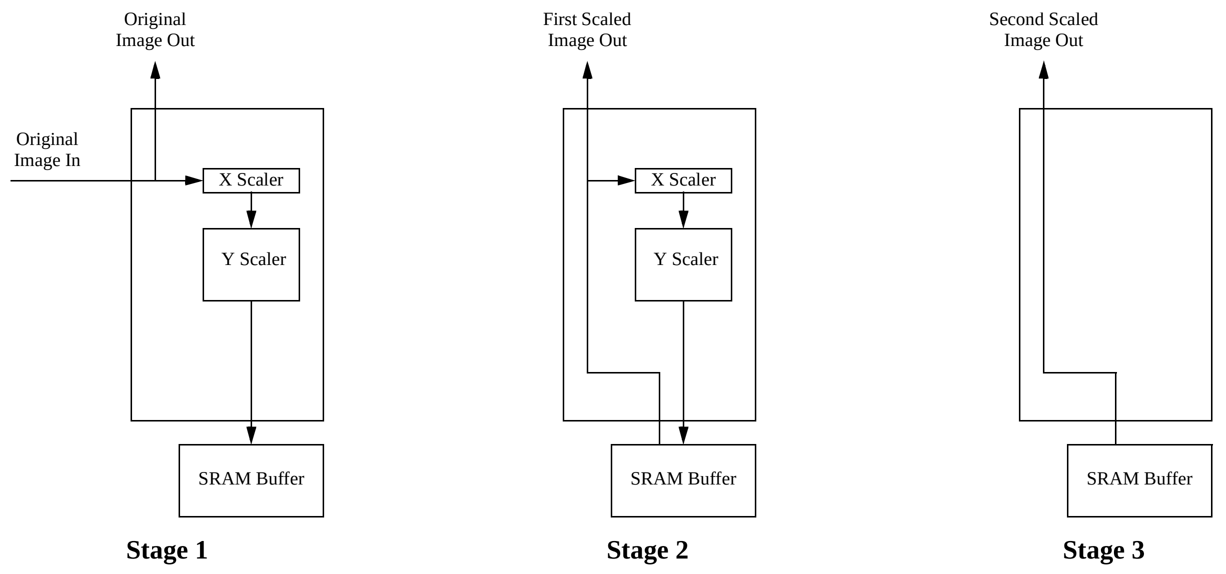

Figure 19: Scaling Unit Processing Stages

two by shrinking its input image twice by a factor of 1.25. From a single original input image these two units together produce nine output images. The smallest of these turns out to be too small to accommodate the 30x32 template after filtering, so it is not processed. We could produce a similar scale range results in less area with a single 1.25 scaling unit, but scaling accuracy would become progressively worse. The two stage process produces a precise power-of-two scale every three steps. This is not very important in the current simple case, but will be more critical for future implementations that use multiple filter scales.

Figure 18 illustrates the basic structure of a scaling unit. There are three major features: an X scaler, a Y scaler, and a memory interface unit to handle access to the off-chip buffer in SRAM. The X and Y scalers together shrink the input using linear interpolation. The structure of the scalers is very similar to the X and Y filtering stages, which we discuss below. The major difference is that the scalers require less bandwidth and thus are smaller. The memory unit stores the scaled image as it arrives from the Y scaler and also retrieves it when needed for output and re-scaling. To produce the required three output images, each unit goes through three stages. Figure 19 shows the flow of data during each of these. First, the unit takes pixels from its inputs and sends these both to the X scaler and to the unit’s output. Once the entire original image has been processed, the unit reads scaled pixels from the buffer and passes these again to both the X scaler and to the unit’s output. In the third and final stage, the last image is read from the buffer and simply sent to the output.

5.5 G2/H2 Filtering

From the scaling unit pixels are passed through separable G2/H2 filters. We have one horizontal and one vertical G2/H2 pair, for a total of four filters. Each filter consists of an X and a Y stage, with the X stage first to take advantage of the row-oriented data coming from the camera. After each stage the filter results are reduced to a signed 8-bit representation which allows efficient storage in memory and has been shown in testing to be an adequate level of accuracy.

5.5.1 Design Tools

The two major design issues common to both X and Y units were the selection of filter coefficients and the construction of an adder pyramid to sum the multiplied pixels. While the filter coefficients are strictly defined in [16], it may be possible to save hardware area by adjusting the coefficients values slightly. We may also save area by selecting the order in which to sum the intermediate results such that the size of the intermediate adders and registers is minimized. To solve these problems we developed three software tools.

The first tool generates a set of G2/H2 basis filters of a specified size and optimizes both the X and Y filter coefficients such that each may be expressed as the sum or difference of two powers of two, with a slight bias towards exact powers of two. To understand why this is useful, we must first examine the cost of various mathematical operations in hardware. Table 5 lists the approximate Altera LCs required for three operations: an 8-bit multiplication, an 8-bit addition, and an 8-bit fixed shift. We can see that additions are much cheaper than multiplications, and fixed shifts

Operation	Logic Cells
8x8-bit Multiplication	121
8-bit Addition	9
8-bit Fixed Shift	0

Table 5: Logic Resources Required for Mathematical Operations

are free. Multiplication hardware, however, is constructed out of fixed shifts and adders; one shift and add for every bit of the multiplier term. If one term in the multiplication is constant, the size of the hardware will shrink roughly in proportion to the number of zeros in the binary representation of the constant. This is because the shift-and-add hardware for a bit fixed at zero is no longer needed. If the constant is a power of two, the multiply becomes just a fixed shift and requires no logic at all. By reducing our constants to be no more complex than a sum or difference of two powers of two, we use no more than one adder or subtractor to calculate a multiplication.

The second and third tools are specific to the X and Y units respectively. Each takes the optimized coefficients and emits a filter hardware description in the Altera AHDL language. In the process, each tool constructs adder pyramids which minimize the size and number of intermediate adders and registers. These tools were extremely useful during the design process. Although the optimization they perform is quite straightforward, they provide some assurance that the implementation is efficient. Equally importantly, they allowed us to change the size of the filters used with little manual re-design.

5.5.2 X Filter Stage

As the X filter is row-oriented and the pixel data is arriving in rows, the X filtering stage is by far the simpler of the two. As Figure 20 shows, it consists of little more than a set of input registers attached to the coefficient and pyramid adders. Pixels are shifted into the input registers to perform the convolution, and X results emerge from the peak of the pyramid.

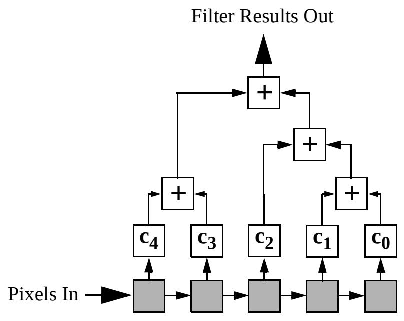

Figure 20: Example Structure of a 5-element X Filter

5.5.3 Y Filter Stage

The Y filter stage receives pixels from its respective X stage and performs a second 1-D convolution. The major problem to overcome when designing the Y filter stage was how to achieve one result per cycle throughput given the incompatible orientations of the X results and the Y filter. The Y filter is a column vector, so for a filter of size $n \times n$ we need n X results organized in a column. The X results, however, arrive in rows. This has two implications: we will need to wait until at least $n - 1$ rows have already arrived before we can use the subsequent X results; and we will need $n - 1$ separate memory reads to collect a column of X results. This problem, called “corner turning”, is quite common. One solution that will work for any size of filter is to buffer the entire set of X results in memory and then read the data back in columns. The major drawback is that it requires considerable memory and introduces a full frame of latency. Fortunately there is a continuum of possible solutions, from full buffering for the largest filters to holding only a few rows in on-chip memory for the smallest. In the current case of a 7×7 filter (after quantization, all border coefficients of the G2 and H2 filters were zero) we were able to use external SRAM and two shifter arrays to produce the required throughput, while storing only six rows of X results and introducing no additional latency.

Figure 21 illustrates the Y filter design. Two 7×7 grids of 8-bit registers perform the required conversion from row-oriented to column-oriented data. Six row-oriented groups of seven pixels are shifted from memory downwards into the grid at the same time as the bottom row is filled with new results coming from the X filter. Once the grid is full the new X results are written to memory and the grids are swapped. While the second grid is filled in an identical manner, the first shifts columns of X results horizontally to the filter pyramid. The process then repeats.

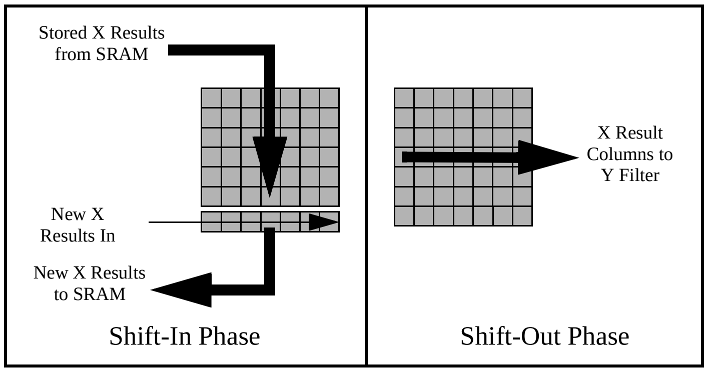

Figure 21: Example of 7x7 Shifter Array Operation

5.5.4 Comparison to Non-Separable Filters

One of the reasons we chose the G2/H2 filter pair was that they are X-Y separable and thus should require less hardware than a non-separable filter with the same throughput. In the implementation each separable filter required approximately 2400 Altera Logic Cells (LCs)[29]. The X and Y filter coefficients and associated adder chains account for around 800 LCs. The remaining 1600 LCs are taken up by the two 7x7 register grids in the Y stage and their control circuitry. Note that majority of the resources are dedicated to reordering the incoming data rather than actually calculating the filter results. If we consider the hardware required for a non-separable filter, it would amount to seven sets of coefficients, eight adder chains, and three 7x7 grids totalling approximately

5200 LCs in all. The separable implementation therefore reduced resource requirements by just over 50% versus non-separable filters. The reason this result is not even more dramatic is that although the move to separable filters reduces the coefficient and adder chain hardware by around 75%, it only reduces the data reordering hardware by 33%.

5.6 QMP Conversion

The QMP conversion units each take the filtering results from one of the G2/H2 pairs and convert them into QMP representation. The final result is quantized into 4 phase bins so we only need to perform two fixed multiplications and three compares, as we describe in Chapter 3. As with the G2/H2 filters, fixed multiplication coefficients are optimized to be the sum or difference of two powers of two, and so the multiplier becomes an adder. To complete the QMP conversion we need to evaluate whether the G2/H2 magnitude is above a fixed threshold. The threshold was set at eight, so we require only two 3-bit squaring units, one 7-bit adder, and three compare operators.

5.6.1 Efficiency of QMP

In the discussion of the QMP format in Section 3.2 we stated that the format substantially contributed to the efficiency of CFA in hardware. To see why this is true, consider the CFA formula for the activation a_{kn} given in (EQ 10) below:

$$a_{kn} = \sum_{s=0}^{N_S - 1} i_{ns} \ln\left(\frac{p^{+}_{kns}}{p^{-}_{kns}}\right) \qquad \text{(EQ 10)}$$

In this formula i_{ns} is an input value representing the probability that input n is currently in state s. In QMP format, the current state is equivalent to the magnitude/phase bin of the response. Since each G2/H2 result is categorized into one and only one bin, one i_{ns} in (EQ 10) has a probability of one and the rest have a probability of zero. If we look again at the activation function, we can see that the computationally expensive sum of products is reduced to a simple selection of one of the $\ln\left(\frac{p^{+}_{kns}}{p^{-}_{kns}}\right)$ values. In hardware, this selection operation will be much more efficient than multiplication.

5.7 Face Detection

The two QMP units pass their results to a Face Detection Unit (FDU), which implements the

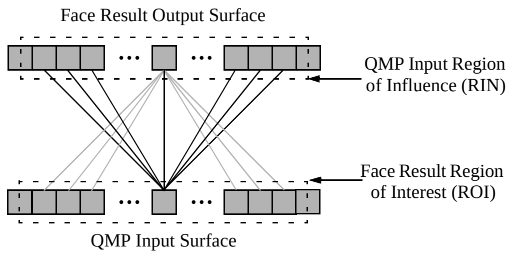
Face Result Output Surface
QMP Input Region of Influence (RIN)
Face Result Region of Interest (ROI)
QMP Input Surface

a. Illustration of face result ROI and QMP input RIN

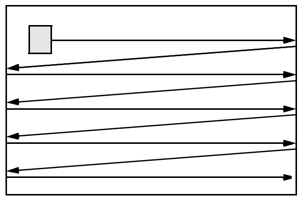

b. Movement of RIN across result surface as QMP rows arrive

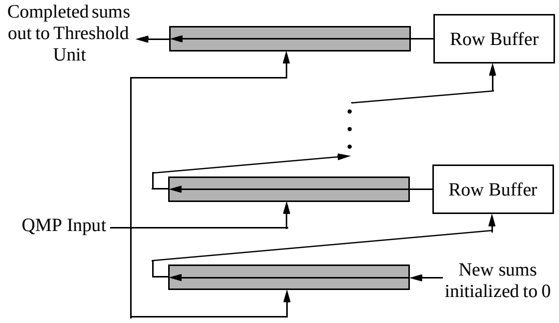
Completed sums out to Threshold Unit
Row Buffer
Row Buffer
QMP Input
New sums initialized to 0

c. FDU Row Unit arrangement

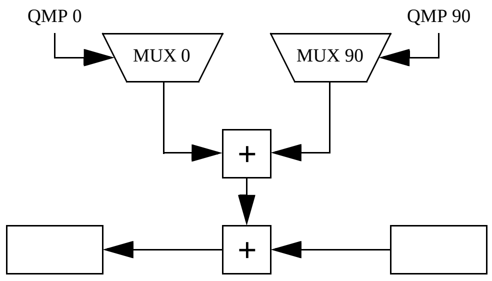

d. Detail of inter-register adder structure

Figure 22: Face Detection Unit Principle and Structure

CFA face classifier. It is by far the largest unit in the system, and is comprised of a front end unit, a set of 32 row units, and a final thresholding unit which are spread among 8 FPGAs in the final system. The front end unit performs minimal buffering of data and detects the end of the current image. The row units together calculate the face likelihood sums. The thresholding unit sets all sums below the face acceptance threshold to zero, and passes the results to the peak detection unit.

5.7.1 FDU Structure

In order to comply with our throughput requirement, the FDU must be able to both consume one QMP value pair and produce one face probability every clock cycle. This design achieves the required throughput by managing the flow of feature activation sums through the hardware such that as soon as a QMP value pair is ready to be processed, all of the activation sums to which it is an input are available in active registers. For each QMP pair there is a region on the face probability output surface consisting of all face probability outputs that the pair affects. This is called the Region of INfluence (RIN) for that pair. Figure 22a illustrates an input's RIN. In this diagram we show simplified 1-D versions of the QMP input surface at the bottom and the face result surface at the top. Each box in the input surface represents one QMP value, and each box in the result surface represents the output of one replicated feature. In solid lines, we show the RIN of the highlighted QMP value. The shape and size of the RIN is the same as the feature scope.

As the FDU receives its input stream of QMP value pairs, it maintains all of the face activation sums that will be affected by the next QMP value - that value's RIN - in a large bank of registers and updates these sums as QMP values arrive. It is instructive to review how the FDU uses the QMP inputs to calculate an activation sum an produce a face probability. The value that the FDU operates on is the activation a_k associated with an output k. This requires the calculation, for each input n, of the activation a_{kn} of output k with respect to input n. These formulas are given below:

$$a_k = b_k + \sum_{n=0}^{N_I - 1} r_{kn} a_{kn} \qquad \text{(EQ 11)}$$

$$a_{kn} = \sum_{s=0}^{N_S - 1} i_{ns} \ln\left(\frac{p^{+}_{kns}}{p^{-}_{kns}}\right) \qquad \text{(EQ 12)}$$

As we discussed in Section 5.6.1, for each input n one i_{ns} has a value of 1.0 and the rest are zero. Each input thus selects of one of the constant $\ln\left(\frac{p^{+}_{kns}}{p^{-}_{kns}}\right)$ values to be added to the overall activation a_k. As a QMP pair arrives, the FDU must update all of the activations in the input's RIN by selecting the appropriate constant for each and adding it to the sum. QMP results arrive at the FDU from left to right in row orientation. This causes the effective current RIN to scan across the face from left to right, returning to the left-hand side and dropping down one at the end of each row as illustrated in Figure 22b. In addition to adjusting the activation values, the FDU must also shift the current RIN to prepare it for the next input.

The FDU row units implement this add-and-shift operation by storing a row of face results in on-chip memory and using a bank of 31 registers connected in a chain by 30 adders. Figure 22c illustrates the arrangement and connection of the row units and shows how results flow through the FDU. The face results in the current RIN are located in the first 30 registers. When a new QMP result arrives, its value is used as a selection signal to each of the adders indicating which of several constant values should be added to each face result. Figure 22d shows this operation in detail. Face results pass through the adders into the next register, thus performing both RIN shifts to the right, the right-most edge is filled with new face results pulled out of local memory into the start of the register bank. As face results arrive at the end of the register bank they are sent upwards to the next row unit and buffered in local memory for the next left-to-right pass. Results emerging from the end of the topmost row unit are complete and are passed to the thresholding unit. Results entering the start of the bottommost row have not been encountered yet and are thus simply zero.

5.7.2 Design Tools

There is significant complexity involved in properly arranging the model coefficients and determining how may bits are required at each stage of the FDU. To aid in this process we created a software tool that loads a model file created by the learning algorithm and emits an AHDL description of the FDU circuitry. The tool first quantizes the floating-point model coefficients into a user-specified number of bits. It then keeps track of the maximum and minimum possible sums at each stage throughout the row units, allocates as much local memory storage as needed, and sizes the adders and registers properly. This tool was extremely useful during development as it can quickly create brand-new circuitry with a different number of coefficient bits or from a model trained using different learning parameters.

5.7.3 An Alternate Design

Although the current FDU structure works well, there is an alternate solution that we initially overlooked. Figure 22a shows in dashed lines the region on the QMP input surface representing all of the inputs used by one face probability output. This is the Region of Interest (ROI) of that output. If a ROI of QMP inputs is buffered and shifted instead of a RIN of face results, the buffered inputs in the ROI can be used as the input selectors to a large adder pyramid that calculates a single face result sum. This structure would perform the same task using less memory, fewer adders, and smaller registers. It would also allow multiple features to share the buffered input values, leading to a more efficient multi-feature implementation. The current design allows the individual row units to be more self-contained than this alternative, but on the whole the alternate design would be preferable for future implementations. Fortunately, the nearly identical shifting structures of the two solutions will make the new approach easy to implement.

5.8 Peak detection

The peak detection unit receives thresholded face probabilities from the FDU and detects peaks in the resulting surface. This is necessary as each face will produce an above-threshold response at more than one location. Two rows of face results are stored in on-chip memory. As new results arrive they are shifted along with the buffered results into a 3x3 grid of comparators. If the center result is greater than or equal to its eight neighbors, the location is counted as a peak and is passed on to the display unit. In practice this method works well, although a single face will sometimes generate multiple peaks at adjacent locations or scale steps.

5.9 Display

The display unit performs three functions: it buffers the incoming image for display, writes the face markings given input from the peak detection unit, and merges and displays the last frame's image and detection results. There are two pairs of buffers, a draw pair and a display pair, with each pair containing one image buffer for the input image and one "overlay" buffer for the detection results. Using two pairs provides double-buffering so that one frame may be displayed while the other is being drawn. Once a new frame is finished the display and draw buffers are "flipped" during the monitor's vertical blank. This avoids the "tearing" of a display image associated with drawing into a buffer at the same time as it is sent to the monitor.

When the results are being displayed, the display unit uses the value of the overlay pixel to determine what is sent to the monitor: if the overlay pixel is zero, the image pixel value is sent; if it is one, a green pixel is sent; otherwise the overlay pixel value is sent. This allows the face area to be marked in a distinct color or even replaced entirely by a pre-set bitmap. Although the image and overlay buffers are currently stored in the same 2 MB memory bank, they are kept distinct so that they may be moved into separate banks if more bandwidth is required. This may occur if the input image resolution is increased in the future.

5.10 Implementation Results

5.10.1 Functionality

The system is implemented and running using 9 boards of a 16-board TM-2a system. Detection is performed over the entire image and at 8 different scales covering a range of nearly 3 octaves. Any number of faces may be simultaneously detected at any location or scale. Figure 23 shows ac-

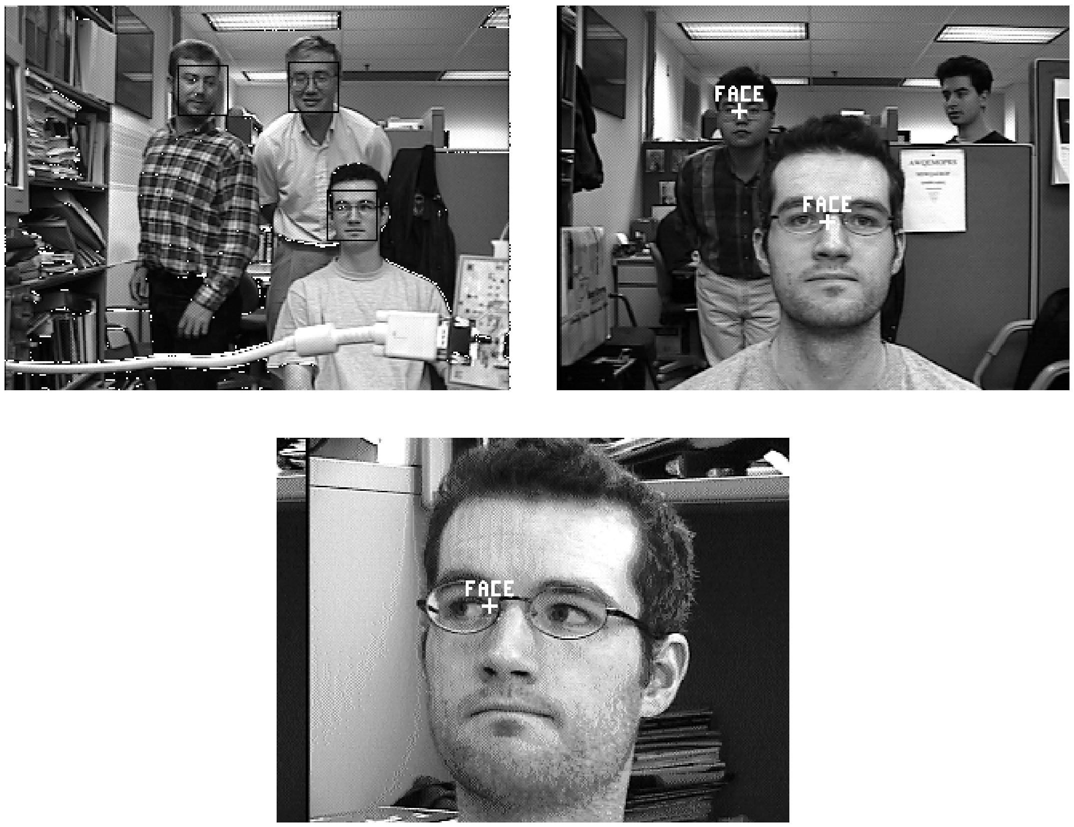

Figure 23: Face Detection Hardware Output

tual output from the face detection hardware as extracted from a memory bank on the TM-2a. These illustrate in particular the considerable face scale range handled by the system and the programmability of the face marker. The image at upper-right also contains a good example of a face not detected due to excessive out-of-plate rotation.

One known error remains unresolved in the current system. If a large number of faces are detected in a small area, the system will halt and requires a reset signal to restart. This situation does not typically occur when an actual face is detected, but rather when a pathological non-face structure generates a large number of false positives. The source of the error has not yet been determined.

5.10.2 Speed

The current system processes the incoming image data at the full frame rate of 30 frames per second. By comparison, a software implementation of the same algorithm would require 32 seconds to perform multi-scale detection on a single frame using a 500 MHz UltraSPARC. This amounts to a speedup of the hardware over the software of approximately 1000 times. This comparison is not particularly relevant, however, as we did not develop our algorithm to be efficient in software. Table 6 lists the reported detection times of actual software face detection algorithms. The times have been approximately normalized to a similar amount of input data and a 500 MHz SPARC processor. We have indicated with an asterisk those methods which use skin tone, motion, or other cues to reduce the number of pixels considered; these cues could also be integrated into our hardware system and would produce similar speed improvements. We can see that the current implementation remains very competitive in any case.

Method	Run Time (s)	Speedup
Lew	~91 seconds	~3000
Rowley et al. (standard)	~180 seconds	~6000
Rowley et al. (“fast”) *	~3 seconds	~90

Table 6: Comparison With Software Methods

5.10.3 Accuracy

Although we have not rigorously tested the accuracy of the hardware system, it is qualitatively lower than that reported during training. This seems to be caused by two factors. First, the face model appears to place undue emphasis on the hairline, which is probably indicative of a bias in the training set. Second, the system requires a surprising amount of contrast on the face and is thus lighting-dependent. This also appears to be the result of a bias in a significant portion of the training set towards lighting directed from above and slightly in front of the face, causing distinct bright patches and very high contrast over the face area. One solution to this problem would be to remove these examples from the training set, but this is problematic as the same images present important variation in hairstyle, face/background polarity, and out-of-plane rotation. The best solution would be to to create new training set of images more representative of the situations we expect to encounter at run time. This would most likely increase the accuracy of the system since the face model would now be more appropriate for the hardware’s operating conditions. It would hopefully have a more dramatic effect on the accuracy reported during training, lowering it to agree better with that observered during operation.

Chapter 6

Conclusions and Future Work

6.1 Conclusions and Contributions

The primary goal of this research was to implement a complex vision task in real-time using a large configurable hardware system. The vision task we chose was face detection. The research proceeded in three stages: we designed, implemented, and tested an object detection framework based on the CFA learning algorithm; we trained a simple face detection system using this framework; and we implemented this system on the Transmogrifier 2a.

We first designed and implemented an object detection framework in software based on the CFA learning algorithm. The framework is a set of parameterized processing steps that can be easily adapted to create a detection system for a specific object, and which are geared towards a hardware implementation.

By developing this framework, we made several contributions. The first is the framework as a whole. Future designers can use it to produce hardware-ready appearance-based detection systems for essentially any object. The second contribution is the QMP format. From a vision perspective, QMP preserves important image texture information while providing excellent invariance with respect to lighting changes. From a hardware perspective, it is very compact and cheap to calculate. The third contribution is the CFA implementation. This is the first application that uses this learning algorithm. During development and testing we verified some of the anticipated benefits of CFA, such as multi-feature decomposition and semi-supervised learning, and showed that the algorithm could accurately decompose an artificial data set containing two independent patterns. We also discovered flaws in the current formulation. The algorithm is unable to learn multiple features from scratch simultaneously, requiring a iterative work-around that is very prone to becoming trapped in local minima. The decomposition found using this iterative method is also very sensitive to regularization. These problems together prevent the algorithm from accurately and efficiently decomposing more complex data. This unfortunately limited the model complexity we could feasibly use for faces to one CFA feature. Nonetheless, the implementation is still very useful and our experiments provide valuable feedback to CFA development.

We next designed and trained a simple face detection system using the object detection framework. We chose a minimal set of four filters and single CFA feature to perform detection. Once trained, the system displayed surprisingly good accuracy results given the simplicity of the face model. We concluded that this was largely due to the QMP representation being an intelligent choice of input space. The major contribution of this stage was the demonstration that the detection framework could produce good accuracy on a complex object even when using very simple operations. Secondary contributions were the training strategies we used to greatly improve both the speed with which the system trained and the resulting accuracy.

In the last stage of research we implemented the face detection algorithm on the Transmogrifier-2a configurable hardware platform. The system detects any number of faces at any location in the image over a three-octave scale range, and runs at the full camera frame rate of 30 frames per second. It requires only nine of the sixteen boards in the TM-2a, leaving nearly half of the system free for future expansion. Compared to the same algorithm in software running on a 500 MHz SPARC processor, the hardware system is approximately 1000 times faster. If we make the more valid comparison to algorithms designed to be efficient in software, we are approximately 3000 to 6000 times faster than systems which restrict themselves to single greyscale images as we do. We remain approximately 90 times faster than systems which use motion and/or colour information to reduce the search space. Although we paid for this increased speed with a longer design process, the time required was only approximately five to ten times over that for a similar software system. These results validate our assertion that large programmable hardware systems are useful platforms for the development of real-time vision applications.

The primary contribution of this stage was, of course, the working system. Any future model improvements gained through CFA development or training modifications can be transferred quickly to hardware using the FDU circuit generation tool. This tool and the filter generation tools are also important contribution. These helped greatly during the design process as they allowed us to quickly incorporate the results of ongoing detection experiments into the hardware design. They also add to the usefulness of the object detection framework by providing a substantial part of the path from a detection system created using the framework to a working hardware version.

6.2 Future Work

There are four major directions of future work to explore based on this thesis. The first and simplest direction is to develop new hardware implementations based on the current face detection algorithm. The second direction is to experiment with various parameters of the face detection algorithm without modifying the basic object detection framework. The third direction is to modify the framework stages and explore new methods including alternate learning algorithms to CFA. The fourth direction is to experiment with the CFA formulation itself.

There are promising research opportunities along each of these directions. One option from the first direction is to add to the hardware system's functionality. For example, it could be extended to handle larger input images, or to handle in-plane rotation in the same way as it currently handles scale. Along the second direction, future work could experiment with using smaller feature scopes that omit the head/background boundary in concert with QMP conversion that does not use phase reflection. This would determine whether the boundary of the head provides useful information and whether phase reflection provides useful lighting invariance. An option from the third direction would be to use the same G2/H2 filtering and QMP conversion but a better understood learning method, such as standard neural networks, to experiment with more complex face models. It would be critical to ensure that the new learning method could gain the same efficiency benefit from using QMP inputs as does CFA, otherwise the size of the detection hardware could easily increase beyond the amount of logic available in the system. Along the fourth direction there is much work to be done. The most critical task is to improve the stability and learning speed of CFA. Without improvement in these areas, it will not be able to perform useful multi-feature decomposition.

References

[1] S. McKenna, S. Gong, J. J. Collins. “Face Tracking and Pose Representation,” *British Machine Vision Conference*, Edinburgh, Scotland, September 1996.

[2] K. C. Yow, R. Cipolla. “Enhancing Human Face Detection using Motion and Active Contours,” In *Proceedings 3rd Asian Conference on Computer Vision*, vol. 1, pp 515-522, Hong Kong, 1998.

[3] K. C. Yow, R. Cipolla. “Scale and Orientation Invariance in Human Face Detection,” In *Proceedings 7th British Machine Vision Conference*, vol. 2, pp 745-754, Edinburgh, 1996.

[4] M. S. Lew. “Information Theoretic View-Based and Modular Face Detection,” *Proceedings of the International Conference on Automatic Face and Gesture Recognition*, Killington Vermont, October 14-16, 1996, pp. 198-203.

[5] C. Han, H. M. Liao, K. Yu, L. Chen. “Fast Face Detection via Morphology-based Pre-processing,” Technical Report TR-IIS-97-001, Academia Sinica Institute of Information Science, January 1997.

[6] B. Moghaddam, A. Pentland. “Probabilistic Visual Learning for Object Detection,“ *International Conference on Computer Vision*, Cambridge, MA, June 1995.

[7] T. Darrell, B. Moghaddam, A. Pentland. “Active Face Tracking and Pose Estimation in an Interactive Room,” *IEEE Conf. on Computer Vision & Pattern Recognition,* San Francisco, CA, June 1996.

[8] P. S. Penev and J. J. Atick. “Local Feature Analysis: A General Statistical Theory for Object Representation,” *Network: Computation in Neural Systems* 7(3), pp. 477-500, 1996.

[9] S. McKenna, S. Gong, Y. Raja. ``Segmentation and tracking using colour mixture models," in Asian Conference on Computer Vision, Hong Kong, 8-11 January 1998.

[10]H. A. Rowley, S. Baluja, and T. Kanade, “Rotation Invariant Neural Network-Based Face Detection”, Computer Vision and Pattern Recognition, 1998, pages 38-44

[11]H. A. Rowley, S. Baluja, and T. Kanade, “Neural Network-Based Face Detection”, IEEE Trans. on Patt. Anal. and Mach. Intell., Vol. 20, No. 1, January 1998.

[12]H. Schneiderman, T. Kanade. “Probabilistic Modeling of Local Appearance and Spatial Relationships for Object Recognition”, IEEE Conference on Computer Vision and Pattern Recognition (CVPR), pp. 45-51. 1998. Santa Barbara, CA

[13]K-K Sung, T. Poggio, “Example-based Learning of View-Based Human Face Detection”, ACCV 1995 and AI Memo #1521, 1572, MIT.

[14]T. K. Leung, M. C. Burl, P. Perona. “Finding Faces in Cluttered Scenes using Random Labeled Graph Matching,” *Fifth International Conference on Computer Vision*, Cambridge, MA, June 1995.

[15]M.C. Burl, T.K. Leung and P. Perona, “Face Localization via Shape Statistics”, Int. Workshop Face and Gesture Recognition, 1995, Zurich, Switzerland

[16]W. T. Freeman and E. H. Adelson, “The design and use of steerable filters”, IEEE Trans. on Patt. Anal. and Mach. Intell., 13(9):891-906, 1991.

[17]E. P. Simoncelli, W. T. Freeman, “The steerable pyramid: A flexible architecture for multiscale derivative computation”, In Second International Conference on Image Processing, Washington, DC, November 1995.

[18]D. Lewis, D. Galloway, M. van Ierssel, J. Rose, P. Chow, “The Transmogrifier-2: A 1 Million Gate Rapid Prototyping System,” in IEEE Trans. on VLSI, Vol. 6, No. 2, June 1998, pp 188-198.

[19]D. Lewis, D. Galloway, M. van Ierssel, J. Rose, P. Chow, "The Transmogrifier-2: A 1 Million Gate Rapid Prototyping System," in FPGA `97, ACM Symp. on FPGAs, Feb 1997, pp. 53-61.

[20]I. Hamer and P. Chow, “DES Cracking on the Transmogrifier 2a,” In Cetin Kaya Koc and Christof Paar, editors, *Workshop on Cryptographic Hardware and Embedded Systems*,

Springer-Verlag Lecture Notes in Computer Science (LNCS 1717), 1999.

[21]A. G. Yee, “Procedural Texture Mapping on FPGAs,” MASc thesis, University of Toronto, 1999.

[22]D. Galloway, “2-D Texture Mapping on TM-2”, Technical Report, University of Toronto, 1996.

[23]S. Brown, J. Rose, "FPGA and CPLD Architectures: A Tutorial," in IEEE Design and Test of Computers, Vol.12, No. 2, Summer 1996, pp. 42-57.

[24]V. Betz, J. Rose, and A. Marquardt, “Architecture and CAD for Deep-Submicron FPGAs”, Kluwer Academic Publishers, 1999.

[25]K. Chia, H. J. Kim, S. Lansing, W. H. Mangione-Smith, and J. Villasenor, “High-Performance Automatic Target Recognition Through Data-Specific VLSI,” in IEEE Transactions on Very Large Scale Integration Systems Vol. 6, No. 3, Sept. 98, page 364-371.

[26]J. Villasenor, B. Schoner, K. Chia, C. Zapata, H. J. Kim, C. Jones, S. Lansing, and B. Mangione-Smith, ”Configurable Computing Solutions for Automatic Target Recognition,” in Proceedings of the IEEE Symposium on FPGAs for Custom Computing Machines, Apr. 1996, pp. 70-79.

[27]M. Rencher, B. L. Hutchings, "Automated Target Recognition on SPLASH 2", in Proceedings of the IEEE Symposium on FPGAs for Custom Computing Machines, April 1997.

[28]R. Petersen, B. L. Hutchings, "An Assessment of the Suitability of FPGA-Based Systems for Use in Digital Signal Processing", In 5th International Workshop on Field Programmable Logic and Applications, pp 293-302, August 1995, Oxford, England.

[29]Altera, “Altera 10K FPGA Databook,” 1996.

[30]A.M. Martinez and R. Benavente, “The AR Face Database,” CVC Technical Report #24, June 1998

[31]D.Hond, L. Spacek, “Distinctive Descriptions for Face processing,” Proceeedings of the 8th British Machine Vision Conference BMVC97, Colchester, England, September 1997, pp.

320-329.

[32]J.H. van Hateren, A. van der Schaaf, “Independent component filters of natural images compared with simple cells in primary visual cortex,” Proc.R.Soc.Lond, 1998, B 265:359-366.

[33]“MIT Media Lab VisTex Database,” http://www-white.media.mit.edu/vismod/imagery/VisionTexture/vistex.html.

Appendix A

This appendix contains an overview of the CFA formulation.

We begin by stating that the output, o_k, of feature f_k is the probability that the feature is present given the input data set D. We then use Bayes Law to express the output in terms of the probability of the data given the presence or absence of the feature:

$$\begin{aligned} o_k &= p(\mathrm{f}_k|D) && \text{(EQ A1)} \\ &= \frac{p(D|\mathrm{f}_k)p(\mathrm{f}_k)}{p(D|\mathrm{f}_k)p(\mathrm{f}_k) + p(D|\bar{\mathrm{f}}_k)p(\bar{\mathrm{f}}_k)} \\ &= \frac{1}{1 + \dfrac{p(D|\bar{\mathrm{f}}_k)p(\bar{\mathrm{f}}_k)}{p(D|\mathrm{f}_k)p(\mathrm{f}_k)}} \\ &= \frac{1}{1 + e^{-a_k}} && \text{(EQ A2)} \end{aligned}$$

where a_k is the feature’s *activation* and is expressed as:

$$\begin{aligned} a_k &= -\ln\left(\frac{p(D|\bar{\mathrm{f}}_k)p(\bar{\mathrm{f}}_k)}{p(D|\mathrm{f}_k)p(\mathrm{f}_k)}\right) \\ &= \ln\left(\frac{p(D|\mathrm{f}_k)p(\mathrm{f}_k)}{p(D|\bar{\mathrm{f}}_k)p(\bar{\mathrm{f}}_k)}\right) && \text{(EQ A3)} \end{aligned}$$

If we make the assumption that the individual members, d_n, of the data set are conditionally independent given the presence or absence of feature k, we can express a_k as a function of their marginal probabilities:

$$a_k = \ln\left(\frac{p(\mathrm{f}_k)}{p(\bar{\mathrm{f}}_k)}\right) + \sum_{n=0}^{N_D - 1} \ln\left(\frac{p(d_n|\mathrm{f}_k)}{p(d_n|\bar{\mathrm{f}}_k)}\right) \qquad \text{(EQ A4)}$$

The negative log probabilities of the data members $\{d_n\}$ represent error terms between the expectations of the feature and the actual data, where lower probabilites produce greater error, and higher probabilities produce lower error. In this case we have two probabilities for each member of the data set: one set conditioned on the presence of the feature, one conditioned on its absence. We therefore also have two error terms: one, E^{+}_{kn},giving the error in the prediction of the data member d_n if the feature is present, the other, E^{-}_{kn}, giving the error if the feature is not present:

$$E^{+}_{kn} = -\ln(p(d_n|\mathrm{f}_k)) \tag{EQ A5}$$

$$E^{-}_{kn} = -\ln(p(d_n|\overline{\mathrm{f}}_k)) \tag{EQ A6}$$

If we consider the component of the activation contributed by d_n, we have:

$$a_{kn} = \ln\left(\frac{p(d_n|\mathrm{f}_k)}{p(d_n|\overline{\mathrm{f}}_k)}\right) \tag{EQ A7}$$

Substituting (EQ A5) and (EQ A6) into (EQ A7), we also have:

$$a_{kn} = (E^{-}_{kn} - E^{+}_{kn}) \tag{EQ A8}$$

which shows that we can express the activation as a difference of error terms. If the feature's presence would introduce less error than its absence, the activation will be positive. Otherwise, the activation will be negative.

Each data member d_n is composed of a probability mass function. For each state s in the sample space there is an associated input probability i_{ns} indicating the likelihood that the input is in that state. The size of the sample space is N_S.

$$d_n = \{i_{n0}, i_{n1}, i_{n2}, \ldots, i_{n(N_S-1)}\} \tag{EQ A9}$$

The feature has two probability mass function for each input, where the probability of d_n being in state s is p^{+}_{kns} if the feature is present and p^{-}_{kns} if it is not present. Since the probabilitiy mass functions must sum to one over the sample space, their values are controlled by a set of lower-level parameters which ensure this property. They are calculated as follows:

$$p^{+}_{kns} = \begin{cases} \dfrac{1}{1 + \sum\limits_{t=1}^{N_S - 1} e^{\alpha_{knt}}} & , s = 0 \\ \dfrac{e^{\alpha_{kns}}}{1 + \sum\limits_{t=1}^{N_S - 1} e^{\alpha_{knt}}} & , s > 0 \end{cases} \tag{EQ A10}$$

$$p^{-}_{kns} = \begin{cases} \dfrac{1}{1 + \sum\limits_{t=1}^{N_S - 1} e^{\beta_{knt}}} & , s = 0 \\ \dfrac{e^{\beta_{kns}}}{1 + \sum\limits_{t=1}^{N_S - 1} e^{\beta_{knt}}} & , s > 0 \end{cases} \tag{EQ A11}$$

Associated with each input is also responsibility r_{kn} indicating the extent to which the feature takes the value of input d_n into account. The formulation of the responsibilites ensures that they are values between 0 and 1:

$$r_{kn} = \frac{e^{\theta_{kn}}}{1 + e^{\theta_{kn}}} \tag{EQ A12}$$

Together, the responsibilities and probability mass functions combine to produce the probabilty of input d_n:

$$p(d_n | \mathrm{f}_k) = \left(\prod_{t=0}^{N_S - 1} (p^{+}_{knt})^{i_{nt}} \right)^{r_{kn}} \tag{EQ A13}$$

$$\ln(p(d_n | \mathrm{f}_k)) = r_{kn}\left(\ln(p^{+}_{kn0}) + \left(\sum_{t=1}^{N_S-1} i_{nt}\alpha_{knt}\right)\right) \quad \text{(EQ A14)}$$

$$p(d_n | \bar{\mathrm{f}}_k) = \left(\prod_{t=0}^{N_S-1} (p^{-}_{knt})^{i_{nt}}\right)^{r_{kn}} \quad \text{(EQ A15)}$$

$$\ln(p(d_n | \bar{\mathrm{f}}_k)) = r_{kn}\left(\ln(p^{-}_{kn0}) + \left(\sum_{t=1}^{N_S-1} i_{nt}\beta_{knt}\right)\right) \quad \text{(EQ A16)}$$

If we substitute the above equations into (EQ A8), we now have:

$$a_{kn} = r_{kn}\left(\ln\left(\frac{p^{+}_{kn0}}{p^{-}_{kn0}}\right) + \left(\sum_{t=1}^{N_S-1} i_{nt}(\alpha_{knt} - \beta_{knt})\right)\right) \quad \text{(EQ A17)}$$

Substituting (EQ A7) into (EQ A4),

$$a_k = \ln\left(\frac{p(\mathrm{f}_k)}{p(\bar{\mathrm{f}}_k)}\right) + \sum_{n=0}^{N_D-1} r_{kn}\ln\left(\frac{p^{+}_{kn0}}{p^{-}_{kn0}}\right) + \sum_{n=0}^{N_D-1} r_{kn}\left(\sum_{t=1}^{N_S-1} i_{nt}(\alpha_{knt} - \beta_{knt})\right) \quad \text{(EQ A18)}$$

This completes the derivation of the feature's activation and output.

Once detection is complete, the ensemble of feature outputs can be considered to be a coding of the input data set in terms of the feature patterns present in the data. In order to determine how well our features code the data, we need to measure the error between the data as predicted by the coding and the original input.

Since more than one feature may be involved, we first need to determine the extent to which any given feature's prediction affects the overall prediction for any given data member. This is controlled by a posterior responsibility $\tilde{r}_{kn}$:

$$\tilde{r}_{kn} = \frac{r_{kn}o_k}{\sum_{j=0}^{N_F-1} r_{jn}o_j} \tag{EQ A19}$$

We also need to calculate the error between a given feature’s prediction and the actual input given the presence or absence of that feature. This is called the posterior error, and it is expressed as:

$$\tilde{E}_{kn} = o_k(E^{+}_{kn}) + (1 - o_k)(E^{-}_{kn}) \tag{EQ A20}$$

We can see that the output of the feature controls the weighting between “present” error and “not present” error, which is intuitively satisfying.

The total prediction error for the ensemble of features for data member d_n is now simply a sum of the posterior errors weighted by the posterior responsibilities.

$$\tilde{E}_n = \sum_{k=0}^{N_F-1} \tilde{r}_{kn}\tilde{E}_{kn} \tag{EQ A21}$$

The total error for the ensemble over the entire data set is a simple sum of the individual data member errors:

$$\tilde{E}_D = \sum_{n=0}^{N_D-1}\left(\sum_{k=0}^{N_F-1} \tilde{r}_{kn}\tilde{E}_{kn}\right) \tag{EQ A22}$$

An update rule for any of the model parameters may be found by taking the partial derivative of the total error with respect to the desired parameter.